GAS FILLED CERENKOV COUNTERS

A. S. VOVENKO, B. A. KULAKOV, M. F. LIKHACHEV, Yu. A. MATULENKO, I. A. SAVIN, and V. S. STAVINSKIĬ

Usp. Fiz. Nauk 81, 453-506 (November, 1963)

INTRODUCTION

CHARGED particles moving in a transparent medium with velocity exceeding the phase velocity of light in this medium emit a unique radiation, part of the spectrum of which lies in the visible region. This radiation was first discovered and investigated by S. I. Vavilov and P. A. Cerenkov in 1934-1938, and was explained theoretically by I. M. Frank and I. E. Tamm in 1937-1939. Many experimental and theoretical investigations* of this phenomenon have been reported since. Let us recall its principal properties.

Cerenkov radiation is characterized by sharp directivity. The radiation angle, the particle velocity, and the refractive index of the medium are connected by the relation†

$$\cos\theta = \frac{1}{n(\lambda)\beta}. \qquad (1)$$

The energy radiated by the particle as it covers a path l in the medium is given by the equation

$$W = 4\pi^2 e^2 l \int_{\beta n > 1} \left[1 - \frac{1}{\beta^2 n^2(\lambda)}\right] \lambda^{-3}\, d\lambda. \qquad (2)$$

If we neglect the dispersion of the refractive index in some wavelength region, that is, if we assume that $n(\lambda_1 - \lambda_2) = \bar{n}$, then we can readily obtain from (2) the number of photons emitted by the particle along the same path:

$$N = 2\pi e^2 (\hbar c)^{-1} l\,(\lambda_1^{-1} - \lambda_2^{-1}) \sin^2\bar{\theta} = B(\lambda_1, \lambda_2)\, l \sin^2\bar{\theta}. \qquad (3)$$

Estimates show that for $\beta \approx 1$ in solid and liquid media, where $\bar{n} \approx 1.5$, some 200—300 photons are produced on 1 cm of path, while in gaseous media, for $\bar{n} \approx 1.01$, the number of photons is about 10.

In spite of this small quantity of light, the Cerenkov radiation can be used to register high-energy charged particles with the aid of so-called Cerenkov counters. Cerenkov counters consist, in general outline, of a medium (radiator) in which light is produced, an optical system which gathers the light, photomultipliers which convert the light into electrical pulses, and electronic apparatus which records these pulses. There are two types of Cerenkov counters—threshold (or integral) and angle (or differential).

Threshold counters have optical systems that are sensitive to light emitted in a wide range of angles, and register particles whose velocities exceed a certain threshold value β_t, determined from relation (1) under the condition that $\cos\theta = 1$:

*Reviews of most investigations can be found in [1,2].

†Here and throughout, unless specially noted, we use the universal symbols: θ—angle between the radiation direction and the direction of motion of the particle, β—particle velocity expressed as a fraction of the velocity of light, n—the refractive index of light in the medium, λ—wavelength in light, etc. These symbols have the same meaning throughout the text. Therefore, to avoid repetition, all symbols are defined when first introduced.

$$\beta_t = \frac{1}{n}. \quad (4)$$

Differential counters register particles whose velocity β_0 satisfies the condition $\beta_0 > \beta_t$ and lies in a narrow interval from β_0 to $\beta_0 + \Delta\beta$. This is attained because their optical systems are sensitive to light emitted in the narrow angle region between θ_0 and $\theta_0 + \Delta\theta$, respectively. The connection between $\Delta\theta$ and $\Delta\beta$, or the velocity resolution of the counter, is obtained by differentiating (1):

$$\frac{\Delta\beta}{\beta} = \mathrm{tg}\,\theta_0\,\Delta\theta = (n^2\beta^2 - 1)^{1/2}\,\Delta\theta. \quad (5)*$$

Obviously, the resolving power of an angle counter will be the better the smaller the angle to which the optical system is set and the narrower its sensitivity region. The best velocity resolution can be obtained when $\Delta\theta$ is on the order of the natural width of the intensity peak of the Cerenkov light.†

Cerenkov counters are frequently used to identify particles by their mass. Since the Cerenkov radiation depends only on the velocity, a unique relation between these two quantities is necessary in order to determine the mass. Such a connection exists in a beam of particles with definite momentum, the discrete velocity spectrum of which corresponds to a discrete set of masses. Consequently, the velocity sensitivity regions of Cerenkov counters can be converted into mass sensitivity regions. The threshold velocity in a given radiator corresponds in this case to a definite mass m_t, and the threshold counters will register all the particles with mass smaller than m_t and velocity larger than β_t. Owing to the one-to-one correspondence between the mass and the velocity, each particle with mass smaller than m_t will radiate light at a definite angle. By adjusting the optical system of a differential counter in suitable manner, it is possible to select the required particles. An analogous result can be obtained also with an optical system set at a constant radiation angle, if the radiator is varied in such a way that the product n remains constant.

By combining threshold and angle counters, it is possible to separate practically all the presently known charged particles. However, at large energies, as $\beta \to 1$ and the difference between particle velocities becomes very small ($\Delta\beta \ll 1$), the selective properties of the Cerenkov counters with solid or liquid radiators are lost. In fact, for $n \sim 1.5$—1.3 the threshold velocity is quite low ($\beta_t \sim 0.7$—0.8), a particle of any mass emits Cerenkov light, and the radiation angles are close to the maximum defined by the equality $\cos\theta_{max} = 1/n$. Naturally, in this case the difference in the radiation angles is very small. From (5) we see that $\Delta\theta \sim \Delta\beta$ as $\beta \to 1$. Since $\Delta\beta \ll 1$, to separate a particle with a definite mass it is necessary to employ optical systems that are sensitive in a very narrow angle interval. The production of such systems involves great technical difficulties [3,4].

Cerenkov counters with gas radiators retain their selective properties up to ultrahigh energies. Indeed, the refractive index of a gas can be made in principle as close to unity as desired, and consequently, it is possible to employ the threshold properties of the Cerenkov radiation at any energy. On the other hand, from (5) with $n \sim 1$ it follows that $\Delta\theta \gg \Delta\beta$, that is, the change of the angle is much larger than the variation in the velocity. Therefore even with a small difference in velocity, it is possible to tune the optical system to a definite angle and register particles with definite mass, provided a sufficient amount of light is produced.

Gaseous media used in Cerenkov counters have one important advantage over solid and liquid media. The refractive index of the gas depends on its density, which varies with the pressure and temperature. This makes it possible to tune the gas counters to different velocity intervals. The connection between the refractive index and the density is given by the well-known Lorentz-Lorenz law

$$\frac{n^2-1}{n^2+2} = \frac{R\varrho}{M}, \quad (6)$$

which in the case of gases can be approximately written in the form

$$n^2 - 1 = \frac{3R\varrho}{M} \quad \text{or} \quad n - 1 = D\varrho, \quad D = \frac{3R}{2M}, \quad (7)$$

where ρ and M are the density and molecular weight of the gas, and R is a constant for the given gas, called molecular refraction.

An essential shortcoming of gas-filled Cerenkov counters is their great length. This is connected with the fact that the radiation angle in a gas, and consequently the intensity, is small. The requirement of high particle registration efficiency makes it necessary to use counters one meter or more in length.

The first experiments aimed at the observation of Cerenkov radiation in gas were made in 1953 by A. Ascoli and Balzanelly and R. Ascoli[5], who observed light flashes when cosmic particles passed through a volume filled with chloroform vapor. The light was registered with a photomultiplier connected for coincidence with a telescope of Geiger counters. In this experiment, however, owing to the large background, there was no complete assurance that the counts produced were due to directed radiation. An improved instrument, a diagram of which is shown in Fig. 1, has permitted the same authors [6] to prove this more convincingly. The radiation produced in a tube 80 cm long filled with dry air at normal temperature and pressure was detected with a photomultiplier, which was brought outside the particle beam in order to reduce the background. The proof that the instrument readings were due to directional radiation was the

*tg = tan.

†The width of the peak is defined as the half-width of the maximum at half the height.

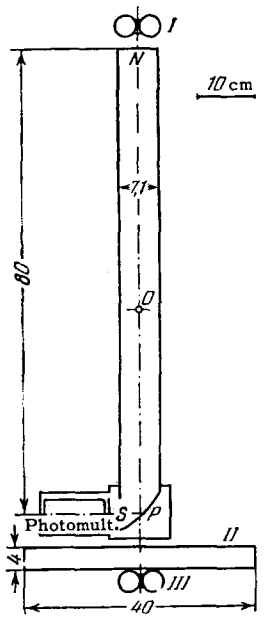

FIG. 1. The counter of Ascoli and Balzanelly. I, II, III–geiger counters; P–parabolic mirror; S–shutter in front of the photocathode of the photomultiplier.

decrease of the count to the background level when the instrument was rotated through 180° about the point O. During the background measurement, the photomultiplier was covered with a shutter.

In one of the test series, the counter yielded the following results:

a) count in normal position with shutter open 1.56 ± 0.2 pulse/hr;

b) count in normal position with shutter closed 0.57 ± 0.2 pulse/hr;

c) count with shutter open and turned through 180° 0.76 ± 0.15 pulse/hr.

The agreement, within the limits of errors, of the two differences (a) – (b) = 0.99 ± 0.28 and (a) – (c) = 0.80 ± 0.25 offers evidence that the effect is due to Cerenkov radiation.

An analogous experiment, but with a more highly perfected setup, was made by Barclay and Jelley, who registered cosmic particles with a counter 6 meters long.

Recently, in connection with the introduction of high-energy particle accelerators, gas-filled Cerenkov counters are widely used in physical experiments. Their operating features are the subject of this article.

In Chapters I and II we present a theoretical analysis of the main characteristics of angle and threshold Cerenkov counters, respectively. Factors which influence the resolution of the counters in velocity and the production of the background in them are considered. In the case of threshold counters, we consider also the dependence of the curve of counter efficiency vs. gas density.

In Chapter III are described optical systems used in gas counters, and the aberrations of such systems are estimated. In Chapter IV are considered gases and methods of obtaining different intervals of refractive indices. Existing constructions of threshold and angle Cerenkov counters are given in Chapter V. In Chapter VI reference material is given for use in the construction of gas counters.

Some of the deductions of the present work are applicable equally well to Cerenkov counters with solid or liquid radiators.

I. DIFFERENTIAL GAS CERENKOV COUNTERS (DGC)

The operation of a differential counter is clear from the foregoing description. The light emitted by the particle at a definite angle to the trajectory of motion is gathered by the optical system and fed to a photomultiplier, which converts it into electrical pulses registered by the electronic apparatus. Since the optical system is sensitive in a narrow interval of emission angles, the amount of light received by the photomultiplier, and consequently the efficiency of the counter, will have a sharply pronounced peak against some background. The form of the efficiency of a differential gas counter as a function of the emission angle can be obtained by plotting, for example, the dependence of the counting rate of particles of a given velocity on the density of the gas. It is obvious that it is similar to the form of the Cerenkov radiation intensity curve and has the appearance of the curve of Fig. 2.

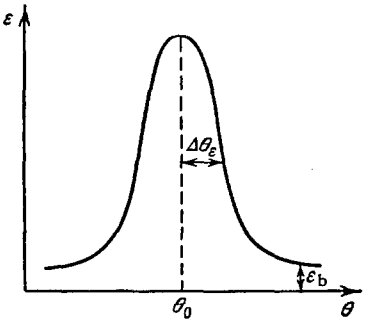

FIG. 2. Schematic form of the efficiency curve of a DGC as a function of the Cerenkov-emission angle.

The width of the efficiency maximum, $\Delta\theta_\varepsilon$, which determines the resolution of the counter in velocity, depends on the width $\Delta\theta_0$ of the radiation maximum and on the sensitivity of the electronic apparatus used to register the photomultiplier pulses.

The factors determining the value of $\Delta\theta_0$ can be combined into three groups:

1) "Angle" factors: angular distribution of the particles in the beam, effects of diffraction of light and multiple scattering of the particle in the material of the counter.

2) "Energy" factors: momentum distribution of the particles in the beam and energy loss by the particle to collision with atoms of the medium.

3) "Technical" factors: dispersion of the refractive index and errors in the optical system.

Each of these phenomena leads to a corresponding broadening of the curve of the Cerenkov radiation intensity.

Depending on the sensitivity of the electronic apparatus, the width of the maximum efficiency of a DGC can be either larger or smaller than $\Delta\theta_0$.

The maximum of the counting efficiency of the DGC as a function of the radiation angle has broad wings, which go over into an approximately isotropic background. The presence of the background is not connected with the nature of the Cerenkov radiation of the primary particle, and is due to different physical phenomena which occur in the walls and in the radiator of the counter. Principal among these are:

a) Cerenkov radiation of the δ electrons produced by the incident particle.

b) Cerenkov radiation of the secondary particles produced as a result of nuclear interaction.

c) Diffraction of light and multiple scattering of the particle at large angles.

d) Molecular scattering of light.

e) Large energy losses by the particle to collisions with the atoms of the medium.

f) Scintillation of the gas and bremsstrahlung.

The size of the background depends also on the surface finish of the optical system.

Let us consider in detail the factors which determine the width of the maximum of efficiency and the background ε_b.

A. WIDTH OF DGC EFFICIENCY MAXIMUM

A1. The maximum angle scatter of the particles in the beam $\Delta\theta_{11}$ and the associated broadening of the radiation-intensity curve are determined either by the geometrical dimensions of the counter itself, or by the telescope of the scintillation counters to which the Cerenkov counter is connected for coincidence. If the diameter of the scintillation counters D is much smaller than the base L, on which they are arranged, then

$$\Delta\theta_{11}\approx\frac{D}{L}.$$

To increase the intensity of the particles, the accelerators are equipped with systems of quadrupole lenses, which make it possible to form almost parallel beams. It is obvious that the divergence of the beam will determine the lower limit of the angular scatter of the particles passing through the Cerenkov counter. Usually this divergence is of the order of $\sim 10^{-3}$ rad.

Even if the particle moves originally parallel to the counter axis, can travel at an angle to it after being scattered on the front wall of the counter or by the atoms of the medium. The problem of the broadening of the Cerenkov intensity curve due to multiple scattering in a medium, with allowance for diffraction, was solved by Dedrik [8]. For small scattering angles, $|\theta_0-\theta|\ll 1$, the distribution of the intensity of the Cerenkov radiation as a function of the angle is shown in Fig. 3, where the ordinates represent the ratio of the intensity at a given angle θ to the maximum possible intensity at an angle $\theta_0=\cos^{-1}(1/n\beta_0)$. The abscissas represent the quantity

$$\delta=\frac{|\theta_0-\theta|\sqrt{2}}{\langle\theta^2\rangle^{1/2}}, \tag{8}$$

where $\langle\theta^2\rangle^{1/2}$ is the mean square angle of multiple scattering of the particle in the counter radiator. In the case when the radiator of the Cerenkov counter is sufficiently thin, $\langle\theta^2\rangle$ can be written in the form [9]

$$\langle\theta^2\rangle=\frac{E_s^2 t}{k^2\beta^2}, \tag{9}$$

where $E_s = 21$ MeV, t is the thickness in radiation units, and k is the momentum of the particle.

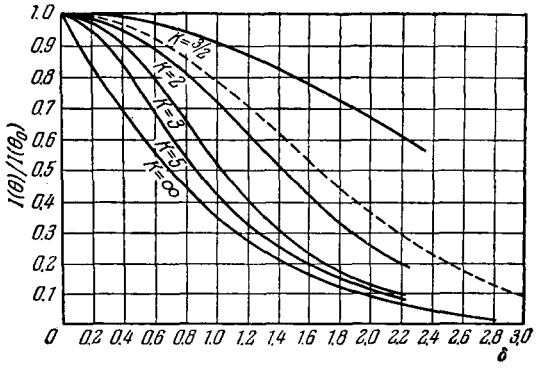

FIG. 3. Angular distribution of the intensity of Cerenkov radiation, calculated with account of diffraction and multiple scattering of the particle. Dashed curve–projection of angular distribution of the particles leaving the radiator.

The parameter K on the curves of Fig. 3 is defined by

$$K=\left(\frac{6\pi}{\sqrt{2}}n\sin\theta_0\frac{l}{\lambda}\langle\theta^2\rangle^{1/2}\right)^{1/3}. \tag{10}$$

A characteristic of the width of the distribution will be chosen to be the angle at which the intensity of light is half the maximum value. Then, on the basis of (8), the broadening of the Cerenkov intensity curve due to multiple scattering, with account of diffraction, amounts to

$$\Delta\theta_{12}=\delta_{1/2}(K)\frac{\langle\theta^2\rangle^{1/2}}{\sqrt{2}}, \tag{11}$$

where $\delta_{1/2}(k)$ corresponds to $I(\theta)/I(\theta_0)=\frac{1}{2}$.

For a gas counter 1.5 meters long, filled with ethylene to a pressure of 30 atm and for a 3-BeV/c particle we have $\Delta\theta_{12}=1.3\times10^{-3}$ rad.

Multiple scattering of particles in the front wall of the counter also increases the angular scatter of the particles passing through the counter, and consequently causes an additional broadening of the light-intensity maximum by an amount $\Delta\theta_{13}$. A measure of

this broadening can be assumed to be the mean-square angle of multiple scattering. Since usually the walls through which the particles pass are thin, $\Delta\theta_{13}$ is determined by relation (9), where now t is the thickness of the wall in radiation units.

The width of the maximum of the Cerenkov radiation, due to all the "angle" effects, is defined by

$$\Delta\theta_1 = \sqrt{(\Delta\theta_{11})^2 + (\Delta\theta_{12})^2 + (\Delta\theta_{13})^2}. \quad (12)$$

With increasing energy, the mean-square angle of multiple scattering decreases both because of the increase in k and because of the decrease in t, so that in order to tune the counter to a larger velocity it is necessary to use a smaller refractive index, that is, a lower gas density. Consequently, with increasing energy, $\Delta\theta_1$ will decrease and tend to a constant limit determined by the divergence of the beam.

A2. If the momentum of the particles passing through the counter lies within a certain interval Δk, then the maximum of intensity of the Cerenkov radiation broadens by an amount $\Delta\theta_2$, which is determined in the case when $\Delta k \ll k$ by the expression

$$\Delta\theta_2 = \frac{1}{\gamma^2 \operatorname{tg}\theta_0} \frac{\Delta k}{k}, \quad (13)$$

where $\gamma = E/m$ and E is the total energy of the particle. We see therefore that $\Delta\theta_2$ is inversely proportional to the tangent of the angle θ_0 to which the optical system is tuned. If the uncertainty of the particle momentum were the only factor leading to a broadening of the radiation intensity curve, then we would obtain by substituting (13) and (5) the limiting Cerenkov-counter velocity resolution, which is independent of the emission angle:

$$\frac{\Delta\beta}{\beta} = \frac{1}{\gamma^2} \frac{\Delta k}{k}. \quad (14)$$

The uncertainty in the momentum of the particles passing through the counter is made up of the momentum scatter of the particles in the beam (Δk_1) and the energy lost to collisions in the radiator (Δk_2). Δk_1 is determined either by calculation or by the method of a current-carrying wire. (We shall show below how to estimate Δk_1 from the curve showing the efficiency of the DGC to a beam in which there are particles with at least two different masses.) Assuming that the energy lost by the particle in the counter are small, we define Δk_2 as follows:

$$\Delta k_2 = \frac{dk}{dl} l,$$

where dk/dl is the momentum loss per unit path.

If we neglect the statistical fluctuations of the energy loss to collision, then we can estimate the broadening of the maximum of the radiation intensity curve due to the particle momentum distribution by means of the relation

$$\Delta\theta_2 = \frac{1}{\gamma^2 \operatorname{tg}\theta} \frac{\sqrt{(\Delta k_1)^2 + (\Delta k_2)^2}}{k}, \quad (15)$$

from which we see that $\Delta\theta_2$ decreases with increasing particle energy.

A3. The dependence of the refractive index on the wavelength of the light causes the radiation of a particle which has a definite velocity to lie in accordance with (1) within a certain angle interval $\Delta\theta_{31}$. From the point of view of increasing the intensity [see relation (3)] it is convenient to use the maximum possible wavelength interval. However, a broadening of the spectral region entails an increase in dispersion, and consequently deteriorates the resolution of the counter in velocity. Differentiating (1), we get

$$\Delta\theta_{31} = \frac{1}{\operatorname{tg}\theta_0} \frac{\Delta n}{n}. \quad (16)$$

The spreading out of the Cerenkov radiation angle as a result of the dispersion of the refractive index, like the momentum distribution of the particles, imposes a limitation on the velocity resolution of the DGC. Substitution of $\Delta\theta_{31}$ in (5) yields

$$\frac{\Delta\beta}{\beta} = \frac{\Delta n}{n}. \quad (17)$$

The dispersion of the refractive indices of gases is considered in Chapter IV.

Any real optical system gathers light emitted in a certain finite angle interval, and at the same time has several errors which lead to a broadening of the maximum of the Cerenkov radiation by an amount $\Delta\theta_{32}$. The simplest systems, their errors, and an estimate of $\Delta\theta_{32}$ are given in Chapter IV.

Summarizing the foregoing, we can assume that the total width of the maximum of the angular distribution curve of Cerenkov light will be characterized by the following relation:

$$\Delta\theta_0 = \sqrt{(\Delta\theta_1)^2 + (\Delta\theta_2)^2 + (\Delta\theta_{31})^2 + (\Delta\theta_{32})^2}. \quad (18)$$

The minimum value of $\Delta\theta_0$ for infinite energy is determined by the divergence of the beam, the dispersion of the refractive index, and by the optical system:

$$\Delta\theta_{0\,\min} = \sqrt{\Delta(\theta_{11})^2 + (\Delta\theta_{31})^2 + (\Delta\theta_{32})^2}.$$

Accordingly, the velocity resolution of a DGC cannot be made arbitrarily high.

B. Background in DGC

The background produces in a counter particles whose velocity is such that they should not be registered by the counter. However, owing to the interaction between these "harmful" particles and the material of the counter, light is produced, part of which lies in the sensitivity region of the optical system of the DGC. Let us consider these interactions.

B1. A charged particle passing through a counter experiences collisions with electrons, as a result of which the recoil electrons (δ-electrons) can acquire an appreciable energy E'. From the conservation laws it follows that

$$E' = 2m_e \frac{k^2 \cos^2\varphi}{[m_e + (k^2 + m^2)^{1/2}] - k^2 \cos^2\varphi} \qquad (c = 1).$$

Neglecting the mass of the electron in the denominator, we obtain

$$E' \approx 2m_e \frac{k^2 \cos^2 \varphi}{m^2 + k^2 \sin^2 \varphi}, \quad (19)$$

where k and m are the momentum and mass of the incident particle, and φ is the angle of emission of the δ-electron relative to the particle trajectory.

If $\varphi = 0$, the electron obtains a maximum energy

$$E'_{max} = 2m_e \left(\frac{k}{m}\right)^2. \quad (20)$$

The probability of collision of particles with electrons was calculated by various authors (see, for example, [10]). For particles with zero spin, the production probability of a δ-electron with energy from E′ to E′ + dE′ on a path l_0 in a gas of density ρ is equal to

$$\Psi(E, E')\,dE' = l_0 \varrho \cdot 2C \frac{m_e}{\beta^2} \frac{dE'}{(E')^2} \left(1 - \beta^2 \frac{E'}{E'_{max}}\right),$$
$$C = 0.15 \frac{Z}{A} \text{ cm}^2/\text{g} \quad (21)$$

For particles with nonzero spin, this formula is approximate. Let us calculate the total number of δ-electrons with energy above threshold

$$N_\delta = \int_{E'_t}^{E'_{max}} \Psi(E, E')\,dE' = 2Cl_0\varrho \frac{m_e}{\beta} \left[\frac{1}{E'_t} - \frac{1}{E'_t}\left(1 + \beta^2 \ln \frac{E'_{max}}{E'_t}\right)\right]. \quad (22)$$

The threshold energy E'_t is determined by the refractive index of the gas. From (4) we obtain

$$E'_t = \frac{nm_e}{\sqrt{n^2-1}} \approx \frac{m_e}{\sqrt{n^2-1}}. \quad (23)$$

If we are interested in the number of δ-electrons produced in a gas whose refractive index corresponds to the threshold of registration with a differential counter of a particle with mass m_0 and velocity β_0, that is, for $n = n_{t_0}$, then we get from (4)

$$n_{t_0}^2 - 1 = \left(\frac{m_0}{k}\right)^2. \quad (24)$$

Substituting expressions (19), (20), (23), and (24) in (22), we obtain

$$N_\delta = 2l_0\varrho C \frac{1}{\beta^2} \frac{m_0}{k} \left[1 - \frac{1}{2} \frac{m_0}{k} \left(1 + \beta^2 \ln \frac{2k}{m_0}\right)\right].$$

For high-energy particles the conditions $\beta \sim 1$ and $m_0/k \ll 1$ are satisfied. Therefore

$$N_\delta \approx 2l_0\varrho C \left(\frac{m_0}{k}\right). \quad (25)$$

Substituting here (7), we obtain ultimately with account of (24)

$$N_\delta \approx 2l_0 C \frac{M}{3R} \left(\frac{m_0}{k}\right)^3.$$

In many cases it is sufficient, in calculations of the probability of registering "harmful" particles via δ-electrons, to determine only the number of these particles, since (25) gives the upper limit of the background due to the collisions with the electrons (naturally, this is correct if $N_\delta \ll 1$ and the efficiency of registration of the δ-electrons is equal to unity). If a rough estimate is not sufficient, a more accurate calculation must be carried out.

The probability ε_{b1} of registration of a "harmful" particle via δ-electrons can be written in the form

$$\varepsilon_{b1} = \int_{\varphi_{min}}^{\varphi_{max}} \Psi(\varphi) P(\varphi)\,d\varphi, \quad (26)$$

where $\Psi(\varphi)\,d\varphi$ is the probability of the formation of δ-electrons in the walls and in the gas of the counter, emitted in the angle interval from φ to $\varphi + d\varphi$ relative to the particle trajectory, and $P(\varphi)$ is the probability of registration of the δ-electrons. We obtain $\Psi(\varphi)\,d\varphi$ from (21) and (19). For simplicity we use an overestimate, assuming that only the factor preceding the parentheses is important in (21). Then

$$\Psi(\varphi)\,d\varphi = 2Cl_0\varrho \frac{1}{\beta^4} \frac{\sin\varphi}{\cos^3\varphi} d\varphi. \quad (27)$$

As will be shown below, if the electronic apparatus is sensitive to pulses corresponding to the knocking out of one electron from the photomultiplier cathode, then $P(\varphi)$ can be written in the form

$$P(\varphi) = 1 - e^{-\bar{N}(\varphi)}, \quad (28)$$

where $\bar{N}(\varphi)$ is the average number of photoelectrons produced on the cathode by the Cerenkov radiation of a δ-electron emitted at an angle φ to the particle trajectory. Allowing for (3), we get

$$\bar{N}(\varphi) = B(\lambda_1, \lambda_2) \sin^2\alpha(\varphi)\, \varepsilon(\lambda)\, l(\varphi)\, \gamma(\varphi), \quad (29)$$

where $\varepsilon(\lambda)$ is the quantum sensitivity of the photocathode, α the angle of Cerenkov radiation of the δ-electron, $\gamma(\varphi)$ the fraction of light entering the sensitivity region of the optical system of the counter, and $l(\varphi)$ the path of the δ-electron in the counter. If the DGC radiator is gas contained in a tube of radius R and length l_0, then by putting $\varphi_0 = \tan^{-1}(2R/l)$, we can assume that

$$l(\varphi) = \begin{cases} \frac{l_0}{2} & \varphi < \varphi_0, \\ \frac{R}{\sin\varphi} & \varphi > \varphi_0. \end{cases} \quad (30)$$

To simplify the calculations we assume that the velocity of the δ-electron is constant, that is, we neglect the ionization and radiation losses and multiple scattering.

Let us determine $\gamma(\varphi)$ (Fig. 4.). Let θ be the angle between the arbitrary generatrix AC of the glow cone of the δ-electron and the direction of the primary particle, DF the line of intersection of the plane passing through the direction of emission of the δ-electron and the direction of the primary particle with the base of the cone, and ξ the angle COF. It is obvious that the fraction of the δ-electron Cerenkov

radiation which enters into the sensitive region $\theta_1-\theta_2$ of the counter optical system is proportional to the length of the arc ab between the generatrices of the cone that make an angle in the interval $\theta_1-\theta_2$ with the direction of motion of the particle, that is,

$$\gamma(\varphi)=2\int_{\xi_1}^{\xi_2}\frac{1}{2\pi}d\xi=\frac{1}{\pi}(\xi_2-\xi_1). \qquad (31)$$

On the basis of Fig. 4 we can show that

$$\cos\xi=\frac{\cos\theta-\cos\varphi\cos\alpha}{\sin\varphi\sin\alpha}. \qquad (32)$$

From the last two relations we obtain

$$\gamma(\varphi)=\frac{1}{\pi}\left(\arccos\frac{\cos\theta_1-\cos\varphi\cos\alpha}{\sin\varphi\sin\alpha}-\arccos\frac{\cos\theta_2-\cos\varphi\cos\alpha}{\sin\varphi\sin\alpha}\right). \qquad (33)$$

A feature of (32) is that $\cos\xi_{1,2}>1$ for certain angles $\varphi>\varphi_{max}$ and $\varphi<\varphi_{min}$. This corresponds to cases when the Cerenkov light from the δ-electron does not enter the sensitive region of the optical system at all. Consequently, $\gamma(\varphi)$ differs from zero only in the angle region $\varphi_{min}<\varphi<\varphi_{max}$. These angles determine the limits of integration in (26).

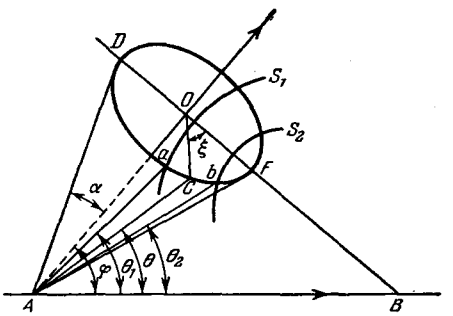

FIG. 4. Illustrating the calculation of the probability of registration of δ-electrons in a DGC. AB—direction of primary particle; AO—direction of emission of the electrons; S_1, S_2—lines bounding the sensitive region of the optical system of the DGC.

Substituting now in (26) the values of all the quantities from (27)—(29) and (33), we obtain a rather cumbersome expression for $\varepsilon_{b1}(\rho, m/k)$—the efficiency of registration of the harmful particle via δ-electrons—as a function of the gas density and the ratio of the particle mass to its momentum:

$$\varepsilon_{b1}\left(\varrho,\frac{m}{k}\right)=\frac{2l\varrho C}{\pi\beta^4}\int_{\varphi_{min}}^{\varphi_{max}}\frac{\sin\varphi\,d\varphi}{\cos^2\varphi}\left[1-\exp\left\{-B(\lambda_1\lambda_2)\varepsilon(\lambda)l(\varphi)\sin^2\alpha(\varphi)\times\left(\arccos\frac{\cos\theta_1-\cos\varphi\cos\alpha(\varphi)}{\sin\varphi\sin\alpha(\varphi)}-\arccos\frac{\cos\theta_2-\cos\varphi\cos\alpha(\varphi)}{\sin\varphi\sin\alpha(\varphi)}\right)\right\}\right], \qquad (34)$$

where $\cos\alpha(\varphi)$, $\sin\alpha(\varphi)$, and $l(\varphi)$ are determined by relations (1), (7), (19), and (30).

Figure 5 shows a plot of $\varepsilon_{b1}(\rho, m/k)$ against the gas pressure, calculated by graphic integration, for a DGC filled with ethylene and having the following characteristics: optical system sensitive in the angle interval from 3.5 to 4.5°, length of counter l_0 = 100 cm, radiator tube radius R = 5 cm. The calculation has been made for m/k = 0.05 for two values of the photomultiplier quantum efficiency: ε_1 = 0.01 and ε_2 = 0.05.

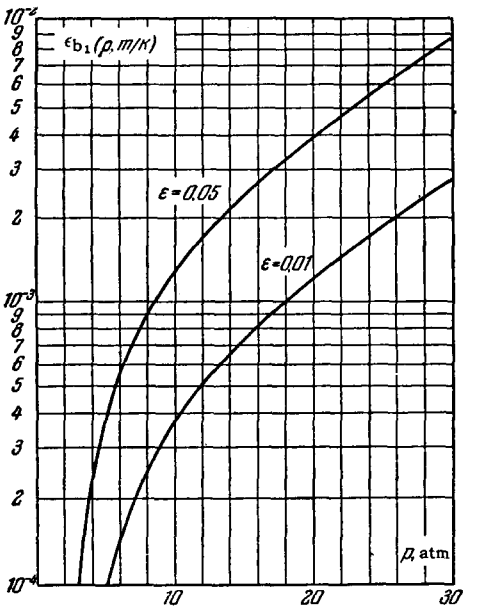

FIG. 5. Probability of registration of a δ-electron by a differential gas Cerenkov counter as a function of the pressure.

Expression (34) gives the most exact estimate of the background produced by the δ-electrons. However, it is not convenient for rapid calculations. In some particular cases it is possible to obtain simpler but approximate formulas. For example, in [13] an estimate is given for the ratio $I(\alpha)/I(\theta_0)$, where $I(\alpha)$ is the intensity of the Cerenkov radiation of the δ electron entering into the sensitive region of the optical system of the DGC, and $I(\theta_0)$ is the intensity of the Cerenkov radiation of the particle to which the DGC is tuned (see Fig. 18 for the diagram of the counter). Only a narrow angle interval was considered for the emission of δ-electrons, the angle between generatrix AF of the cone and the particle trajectory being in the interval from θ_1 to θ_2 (see Fig. 4), that is, $\Delta\varphi\sim\Delta\theta$.

Assuming that all the angles θ_1, θ_2, θ_0, and α are small, $\alpha>\theta_0$, and $\Delta\theta=\theta_1-\theta_2\ll\theta_0$, we get

$$\frac{I(\alpha)}{I(\theta_0)}=\frac{\alpha^2}{\pi\theta^2}\sqrt{\frac{2\theta_0\Delta\theta}{\alpha(\alpha-\theta_0)}}$$

and

$$\Psi(\alpha-\theta_0)\,\Delta\theta = 2l\varrho C(\alpha-\theta_0)\,\Delta\theta. \quad (35)$$

This approximation is justified for the given counter construction, where the angle to which the optical system is tuned is close to the maximum angle of the Cerenkov radiation. Expressions (35) do not depend on the energy and on the mass of the incident particle.

Since the counter efficiency depends on the sensitivity threshold of the electronic apparatus, it is obvious that the higher the threshold, the less probable is the registration of "harmful" particles by means of δ-electrons.

B2. A charged particle with velocity such that it should not be registered by the DGC can enter into a nuclear interaction in the walls or the gas of the counter and be registered as a result. In view of the insufficient information on the angular and energy distributions of the secondary particles, and also in view of the complexity of the calculation, we shall attempt only to obtain the order of magnitude of the background resulting from nuclear interactions, and the character of its dependence on the energy of the primary particle.

If the energy of the incident particle is sufficiently high, then several secondary particles may be produced as a result of the nuclear interaction, and it is known that their angular distribution has a maximum in the forward direction. We shall assume that, with probability close to unity, one of the produced particles has a velocity to which the differential counter is tuned. In this case the probability ε_{b2} of recording the nuclear interaction is determined by the probability with which one of the secondary particles will be recorded by the other counters to which the DGC is connected for coincidence. We can assume approximately that ε_{b2} is determined by the relation

$$\varepsilon_{b2} = \frac{dN}{d\Omega}(0)\,\Delta\Omega, \quad (36)$$

where $\frac{dN}{d\Omega}(0)$ is the distribution of the secondary particles at an angle 0° in the laboratory system, and $\Delta\Omega$—solid angle of the telescope in which the DGC is connected. We shall write for the distribution of the secondary particles

$$\frac{dN}{d\Omega}(0) = \overline{m}\,\frac{d\sigma_\gamma}{d\Omega}(0)\,x = \frac{\overline{m}\sigma_t^2 k^2 x}{16\pi^2},$$

where $\overline{m}$—average multiplicity of the secondary particles, $\frac{d\sigma_\gamma}{d\Omega}(0)$—differential cross section of the cross section of the elastic scattering at angle 0°, σ_t—total cross section of interaction of the primary particles, and x—thickness of the counter (nucleons per cm^2). Under these assumptions, the DGC background due to the nuclear interactions will increase quadratically with increasing particle momentum. Estimates show that when the particle momentum is ~ 10 BeV/c we have $\varepsilon_{b2} \sim 10^{-5}$.

B3. Multiple scattering of the "harmful" particle through large angles can be a source of false DGC counts. The distribution of the intensity of Cerenkov radiation at large scattering angles, as well as for small angles, was obtained by Dedrik [8]. Estimates show, however, that the background due to this effect can be neglected.

B4. When light passes through a medium, scattering connected with the density fluctuations—local condensations and rarefactions of the molecular system—occurs.

The intensity of light $I_S(\xi)$ scattered per unit solid angle in a direction ξ on passing a path l through the medium is given by the Rayleigh formula (see, for example, [11])

$$I_S(\xi) = \frac{(2\pi)^2}{\lambda^4}\, l\, \frac{(n-1)^2}{N_1} \sin^2\xi I_0, \quad (37)$$

where I_0 is the total intensity of the incident light, N_1 is the number of molecules per cm^3. The total intensity I_S of the scattered light is obtained by integrating (37) over the entire solid angle:

$$I_S = \frac{16\pi^3}{3\lambda^4}\, l\, \frac{(n-1)^2}{N_1} I_0. \quad (38)$$

Let us estimate γ_S—the fraction of the Cerenkov light of the "harmful" particle entering as a result of scattering into the sensitivity region of the optical system of the DGC. For simplicity we assume that the scattered light has at the same total intensity not the distribution given by (37) but an isotropic distribution

$$I = \frac{I_S}{4\pi}. \quad (39)$$

Then

$$\gamma_S = \frac{I_S}{I_0}\,\frac{\Delta\Omega}{4\pi} = \frac{16\pi^3}{\lambda^4}\,\frac{l(n-1)^2 M}{N_1}\,\frac{2\pi\sin\theta_0\,\Delta\theta}{4\pi}, \quad (40)$$

where $\Delta\Omega$—solid angle of the sensitive region of the counter. In a counter of length ~ 1 meter with a sensitivity region from 3 to 5°, filled with ethylene to a pressure of 30 atm, we have $\gamma_S \sim 10^{-5}$.

The transition to isotropic distribution of the scattered light leads to an overestimate in the region of small scattering angles. From (37) and (39) we see that $I \geq I_S(\xi)$ up to an angle ξ_0 determined by the condition $\sin^2\xi_0 = 1/3$, that is, $\xi_0 \sim 35°$. Since angles smaller than 35° are used in gas counters, this approximation is correct for such counters.

From the foregoing estimate it is clear that the contribution of the molecular scattering to the production of the DGC background will be negligibly small.

B5. The particle energy loss in collisions with atomic electrons has a statistical character, and, as shown L. D. Landau [12], the probability of a large loss as a result of single collisions can be appreciable. Consequently, in a beam with a given momentum k_0, a harmful particle with mass $m_1 < m_0$ moving with velocity $\beta_1 > \beta_0$ can lose part of the energy

in such a way that its new velocity β_1' is equal to the velocity of the particle β_0 to which the DGC is tuned. It is obvious that this effect begins to manifest itself starting with a value of particle momentum k such that $\beta_1' = \beta_0$ is realized when the maximum possible energy is transferred to the electron. From the condition $\beta_1' = \beta_0$ it follows that

$$\frac{m_0}{k_0} = \frac{m_1}{k_0 - k_{e\,\max}}.$$

At large energies $k_{e.max} \approx E_{max}$ [see (20)]. Taking this into account, we find that the probability of single collisions with large energy loss must be taken into account for a beam of particles whose momentum satisfies the condition

$$k_0 \geqslant \frac{m_1^2}{2m_e}\left(1 - \frac{m_1}{m_0}\right).$$

If m_0 is the mass of a K meson and m_1 is the mass of a π meson, then $k_0 \geq 14$ BeV/c.

B6. The scintillation of the gas and bremsstrahlung of the primary particle will be considered in Chapter III. Getting ahead of ourselves, we shall state that these phenomena make a negligible contribution to the production of the DGC background.

The foregoing analysis shows that of all the physical processes which lead to the production of a background in a DGC, the principal ones are collisions of the primary particle with atomic electrons and nuclear interactions. The remaining processes are apparently of purely academic interest for DGC.

C. Determination of the Mass and Momentum of Beam Particles with the Aid of a DGC

If we know the angle at which the efficiency of registration with a differential counter of particles of a given mass has a maximum, then the momentum of the particles of the beam can be readily determined:

$$k = \frac{m_1}{\sqrt{(n_1^2 - 1) - n_1^2 \sin^2\theta_0}}. \qquad (41)$$

Here n_1 is the refractive index of the gas, corresponding to the maximum efficiency of the DGC to a particle with mass m_1. When the angle is not known exactly, the error in the determination of k may turn out to be appreciable:

$$\frac{\Delta k}{k} = \gamma^2 \operatorname{tg}\theta_0\, \Delta\theta, \qquad (42)$$

where $\Delta\theta$—inaccuracy in the angle θ_0.

This difficulty can be circumvented if the beam contains particles of different masses: pions, K-mesons, protons. Knowing the dependence of the counting efficiency of these particles on the gas density, we can derive relations analogous to (41) for each maximum. Then, eliminating the angle from two equations, we obtain

$$k = \sqrt{\frac{m_2^2 n_1^2 - m_1^2 n_2^2}{n_2^2 - n_1^2}}, \qquad (43)$$

where n_1 and n_2 are the refractive indices at the maxima of efficiency for the masses m_1 and m_2 respectively. Here

$$\frac{\Delta k}{k} \approx \frac{n_1 n_2 \sqrt{n_1^2 + n_2^2}\,(m_2^2 - m_1^2)}{k^2 (n_2^2 - n_1^2)^2}\,\Delta n,$$

Δn—error in the determination of the refractive index corresponding to the maximum efficiency.

If we eliminate the angle and momentum from three relations of the type (41), we obtain a condition connecting the masses of the beam particles

$$m_2^2 (n_3^2 - n_1^2) = m_3^2 (n_2^2 - n_1^2) + m_1^2 (n_3^2 - n_2^2). \qquad (44)$$

From this we can determine the mass of one of the particles, knowing the value of the two others. For example, if m_1 and m_2 are the masses of a pion and proton respectively, then by measuring the refractive indices $n_{1,2,3}$ with accuracy $\Delta n_{1,2,3} \sim 10^{-5}$, we can determine the K-meson mass with an error of ~ 1 MeV.

The dependence of the widths of the DGC efficiency maxima on the gas density (that is, on $n^2 - 1$) enables us to determine the variance of the momentum distribution of the particles in the beam, that is, in some sense, to solve the inverse of the problem treated in Sec. A2. The variance of the efficiency $\sigma_\varepsilon^2(n^2 - 1)$ consists of the variance of the angular resolution $\sigma^2(\theta)$ and the variance of the momentum distribution $\sigma^2(k)$:

$$\sigma_\varepsilon^2 (n^2 - 1) = \left[\frac{\partial (n^2 - 1)}{\partial \theta}\right]^2 \sigma^2(\theta) + \left[\frac{\partial (n^2 - 1)}{\partial k}\right]^2 \sigma^2(k). \qquad (45)$$

From (1) we have

$$\frac{\partial (n^2 - 1)}{\partial \theta} = 2n^2 \operatorname{tg}\theta, \qquad \frac{\partial (n^2 - 1)}{\partial k} = -2n^2 \frac{1}{\gamma^2 k}.$$

Equations (45) for the two maxima of efficiency yield

$$\sigma^2(k) = \frac{\cos^4\theta k^6}{4} \frac{n_1^4 \sigma_\varepsilon^2 (n_2^2 - 1) - n_2^4 \sigma_\varepsilon^2 (n_1^2 - 1)}{n_1^4 m_2^4 - n_2^4 m_1^4}. \qquad (46)$$

For small angles θ and for $n_{1,2}$ close to unity we get

$$\sigma^2(k) \approx \frac{k^6}{4} \frac{\sigma_\varepsilon^2 (n_2^2 - 1) - \sigma_\varepsilon^2 (n_1^2 - 1)}{m_2^4 - m_1^4}. \qquad (47)$$

II. THRESHOLD GAS CERENKOV COUNTERS (TGC)

As was already noted, the directivity property of Cerenkov radiation does not play an important role in TGC. In practice this is manifest in the fact that counters of this type have optical systems with a constant light-gathering efficiency in some rather broad angle interval.

The dependence of the efficiency of registration with a threshold counter of particles with definite velocity β_0 (or with definite mass m_0 in a beam of particles with momentum k) on the gas density has the form shown in Fig. 6. The density ρ_t corresponds to a "threshold" refractive index (4), which can be expressed in the form (24). With increasing density [on the basis of (6), (3), and (1)], the glow

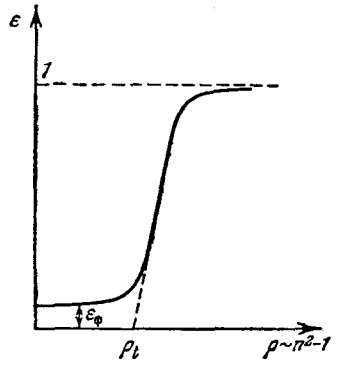

FIG. 6. Schematic form of the curve of the TGC efficiency as a function of the gas density.

angle and the quantity of radiated light increase. Accordingly (if the optical system has constant light-gathering efficiency, starting with 0°), the amount of light incident on the photomultiplier increases, and the counter efficiency approaches unity.

For a given amount of light produced by the charged particle in the gas, the TGC efficiency depends on many factors, which can be broken up into three groups.

A. Apparatus factors:

1) coefficient of gathering of light by the optical system; 2) quantum yield and gain of photomultiplier; 3) sensitivity of the electronic apparatus; 4) noise pulses of the photomultiplier.

B. "Beam" factors:

1) momentum scatter of the particles of given mass m_0; 2) admixture of particles with different masses.

C. Factors dependent on the medium:

1) Cerenkov radiation of δ-electrons; 2) bremsstrahlung of primary particles; 3) gas scintillation.

The efficiency of the TGC in the region $\rho < \rho_t$ is due essentially to factors of the third group, which are responsible for the production of the counter background ε_b. Part of the background is due also to the presence in the beam of lighter particles, with velocity $\beta > \beta_0$, and to random coincidences connected with the photomultiplier noise.

Factors of the first and second groups determine the dependence of the TGC efficiency on the gas density in the region $\rho > \rho_t$. Let us consider each group in detail.

A. Apparatus Factors which Influence the Efficiency of Threshold Counters

It is obvious that the efficiency of the counter depends on the average number $\overline{N}$ of the photoelectrons knocked out by the light from the photomultiplier cathode. The average number of photoelectrons is proportional to the intensity of the Cerenkov radiation, to the light gathering coefficient $\eta(\theta, l)$, and to the quantum sensitivity of the photomultiplier cathode $\varepsilon(\lambda)$:

$$\overline{N} = 2\pi\alpha \int_{\lambda} \int_{L} \sin^2\theta \eta(\theta, l)\, \varepsilon(\lambda)\, \lambda^{-2}\, d\lambda\, dl. \tag{48}$$

If the dispersion of the medium and the deceleration of the particles in it are small, so that the change in the angle of radiation is insignificant, we can write for glow angles at which the light gathering is constant

$$\overline{N} = A \sin^2\theta, \tag{49}$$

where $A = 2\pi\alpha \int_L \int_\lambda \eta(l)\varepsilon(\lambda)\lambda^{-2}\, dl\, d\lambda$ is a constant for each counter, determined by the light gathering and the quantum sensitivity of the photomultiplier. The probability of photoelectron production is described by binomial distribution law, with a mean value equal to the quantum sensitivity of the photocathode $\varepsilon = (\overline{N/M})$, and with a variance $\varepsilon(1-\varepsilon)/M$, where N and M are the numbers of photoelectrons and photons, respectively. We see therefore that the distribution of the number of photoelectrons has a mean value $\overline{N} = \varepsilon\overline{M}$ and a variance $\varepsilon(1-\varepsilon)\overline{M}$. Since the quantum sensitivity is small, that is, $\varepsilon(1-\varepsilon)\overline{M} \approx \overline{N}$, we can assume that the photoelectrons have a Poisson distribution

$$W(N, \overline{N}) = \frac{\overline{N}^N e^{-\overline{N}}}{N!}. \tag{50}$$

The statistical distribution of the photoelectrons on the photomultiplier cathode is transformed at its output into a spectrum of pulses of different amplitudes, the counter efficiency depending on the magnitude of the amplitude. Denoting by P(N) the probability with which the electronic apparatus records the pulses corresponding to the knocking out of N electrons from the cathode, and bearing in mind that P(0) = 0, we write for the TGC efficiency

$$\varepsilon = \sum_{N=0}^{\infty} W(N, \overline{N}) P(N)$$
$$= 1 - W(0, \overline{N}) - \sum_{N=1}^{\infty} W(N, \overline{N})[1 - P(N)]. \tag{51}$$

If we can set the threshold of the electronic apparatus in such a way that it registers the pulses corresponding to N electrons from the photomultiplier cathode and does not register pulses corresponding to N − 1 electrons, then

$$P(N') = 0 \quad \text{for} \quad N' \leqslant N-1,$$
$$P(N') = 1 \quad \text{for} \quad N' \geqslant N.$$

Then it follows from (51) that

$$\varepsilon = 1 - e^{-\overline{N}} - \sum_{N=1}^{N-1} \frac{\overline{N}^N}{N!} e^{-\overline{N}}.$$

For the sensitivity of the electronic apparatus corresponding to the knocking out from the photocathode of one electron we have

$$\varepsilon_1 = 1 - e^{-\bar{N}}, \quad (52)$$

for two electrons

$$\varepsilon_2 = 1 - e^{-\bar{N}}(1 + \bar{N}) \text{ etc.} \quad (53)$$

The spectrum of the pulses at the output of the photomultiplier depends not only on the distribution of the photoelectrons but also on the fluctuations of the gain of the photomultiplier, which is determined essentially by the fluctuations in the first stages (see [1], p. 115). The spreading of the pulse spectrum due to the fluctuations causes the probability of appearance of a pulse at the output of the photomultiplier to remain always finite. Therefore even if the electronic apparatus has a zero threshold, P(N) is never exactly equal to unity. Consequently, the statement that the apparatus has a sensitivity of one photoelectron, and in the use of relation (52) in this connection, is a certain idealization. This idealization can be justified if $1 - P(1) \ll 1$. The statements that the sensitivity of the apparatus corresponds to 2, 3, etc., photoelectrons and the use of relations (53), etc., are apparently even cruder approximations.

In the analysis that follows we shall assume that the gains of the first stages are sufficiently large and that the threshold of the electronic apparatus is sufficiently low, so that the registration efficiency is

$$\varepsilon = 1 - e^{-\bar{N}},$$

or

$$-\ln(1-\varepsilon) = \bar{N}. \quad (54)$$

Using (1) and (49), we express the average number of the photoelectrons in terms of the refractive index and the mass-to-momentum ratio of the particle:

$$\bar{N} = \frac{A}{n^2}\left[(n^2-1) - \left(\frac{m}{k}\right)^2\right] \approx A\,[(n^2-1) - (n_t^2-1)]. \quad (55)$$

Substituting (55) and (7) in (54), we obtain the connection between the efficiency of the TGC and the gas density

$$\ln(1-\varepsilon) = \frac{3AR}{M}(\varrho - \varrho_t). \quad (56)$$

B. Influence of the Beam Particle Velocity Distribution on the Form of the TGC Efficiency Curve

The velocity spectrum in a particle beam can be due to two causes: the momentum scatter and the presence of particles with different masses.

The velocity spectrum can either be continuous or consist of individual lines of finite width.

Let the probability of the particle having a velocity in the interval between β and $\beta + d\beta$ be equal to $W(\beta)d\beta$. Any velocity β can be set in correspondence with a threshold refractive index or a function of the refractive index.

$$\beta = \frac{1}{n_t} = \frac{1}{\sqrt{1+\Delta_t}},$$

where $\Delta_t = n_t^2 - 1$. The velocity distribution can be transformed into a distribution that depends on Δ_t:

$$W(\beta)\,d\beta \to W(\Delta_t)\,d\Delta_t.$$

Let us consider the case when the efficiency of the TGC is determined by relation (52), where $\bar{N} = (A/n^2)(\Delta - \Delta_t) \approx A(\Delta - \Delta_t)$. Then the efficiency of the counter as a function of Δ, in a particle beam with distribution $W(\Delta_t)$, is equal to

$$\varepsilon(\Delta) = \int_0^{\Delta} W(\Delta_t)\,[1 - e^{-A(\Delta-\Delta_t)}]\,d\Delta_t. \quad (57)$$

Let the distribution $W(\Delta_t)$ be bounded:

$$W(\Delta) = 0 \text{ when } \begin{cases} \Delta < \Delta_{t\,\min}, \\ \Delta > \Delta_{t\,\max}. \end{cases}$$

In this case the Δ axis can be broken up into three regions:

1) $\Delta < \Delta_{\min}$. Naturally, the Cerenkov-radiation efficiency of the TGC is equal to zero in this region, since the refractive index is below threshold for particles with maximum velocity.

2) $\Delta_{\min} < \Delta < \Delta_{\max}$. This region corresponds to a case when the refractive index is still lower than threshold for some particles. The counter efficiency here is

$$\varepsilon(\Delta) = \int_{\Delta_{\min}}^{\Delta} W(\Delta_t)\,[1 - e^{-A(\Delta-\Delta_t)}]\,d\Delta_t$$

$$= [1 - e^{-A(\Delta-\bar{\Delta})}] \int_{\Delta_{\min}}^{\Delta} W(\Delta_t)\,d\Delta_t, \quad (58)$$

where $\bar{\Delta}$ is the mean of $\Delta_{\min}$ and Δ.

3) $\Delta > \Delta_{\max}$, that is, the refractive index is larger than threshold for the slowest beam particles. For this region

$$\varepsilon(\Delta) = 1 - e^{-A\Delta} \int_{\Delta_{\min}}^{\Delta_{\max}} W(\Delta_t)\,e^{A\Delta_t}\,d\Delta_t = 1 - e^{-A(\Delta-\bar{\Delta})}, \quad (59)$$

where $\bar{\Delta}$ is the mean of $\Delta_{\min}$ and $\Delta_{\max}$.

From the $\varepsilon(\Delta)$ curve in the third region we can determine A and the average threshold refractive index, and consequently also the particle velocity[14,15], extrapolating to zero the dependence of $\ln(1-\varepsilon)$ on Δ. The abscissa intercept gives the value of $\Delta = \bar{\Delta}$, and the slope will give the value of A.

In principle, if the $\varepsilon(\Delta)$ curve is known with sufficient accuracy and there are no other effects to distort the form of the TGC efficiency curve, we can find not only the average momentum, but the entire velocity distribution of the particle. Differentiating (57) twice with respect to Δ, we obtain

$$W(\Delta_t) = \frac{d\varepsilon}{d\Delta} + \frac{1}{A}\frac{d^2\varepsilon}{d\Delta^2}. \quad (60)$$

C. Efficiency of TGC Below the Radiation Threshold

C1. Let us estimate the probability of registration of a particle by means of δ-electrons. As for the

DGC, we assume that this probability ε_{b1} is given by (26)

$$\varepsilon_{b1} = \int_{E_t}^{E_{max}} \Psi(E, E') P(E') dE',$$

where $\Psi(E, E')dE'$ is the probability of production of a δ-electron with energy between E' and E' + dE' (22), and P(E') is the probability of its registration by the TGC (52). To estimate ε_{b1} we made several simplifying assumptions, which can only make this quantity larger.

1) We assume that in (52)

$$\overline{N} = A' \sin^2 \theta,$$

where A', generally speaking, depends on the length of the δ-electron path in the counter gas, but we assume that it is constant.

2) The δ-electron velocity is assumed equal to unity, and in this case E' = k'. Then, taking (55) into account, we get

$$\overline{N} = A' \left[\Delta - \left(\frac{m}{E'} \right)^2 \right], \quad \Delta = n^2 - 1. \tag{61}$$

3) We assume the maximum δ-electron energy to be infinite.

4) We represent the δ-electron registration probability P(E') in the form

$$P(E') = \overline{N} \qquad 0 \leqslant \overline{N} < 1,$$
$$P(E') = 1 \qquad \overline{N} \geqslant 1.$$

After these assumptions we write ε_{b1} in the form

$$\varepsilon_{b1} = \int_{E_t}^{E_1} \Psi(E, E') \overline{N} dE' + \int_{E_1}^{\infty} \Psi(E, E') dE', \tag{62}$$

where E_t and E_1 are obtained from (61) for $\overline{N} = 0$ and $N = 1$, respectively. Since $\Delta \ll 1$ in gas counters, we get

$$E_t \approx \frac{m_e}{\sqrt{\Delta}}, \quad E_1 = \frac{m_e}{\sqrt{\Delta - \frac{1}{A'}}}. \tag{63}$$

Substituting (22) and (61) in (62) and integrating within the limits (63), we obtain:

1) When $A'\Delta \leq 1$, that is, when $\overline{N} \leq 1$ and it is necessary to take only the first integral

$$\varepsilon_{b1} = 2C\varrho l \frac{2}{3} A' \Delta^{3/2}; \tag{64}$$

2) when $A' \geq 1$

$$\varepsilon_{b1} = 2C\varrho l \cdot \frac{2}{3} A' \Delta^{3/2} \left[1 - \left(1 - \frac{1}{\Delta A'} \right)^{3/2} \right]; \tag{65}$$

3) when $A'\Delta \gg 1$ we find from (65), by expanding in a series, that the probability of registration of a particle by means of δ-electrons in the TGC is equal to the total probability of production of δ-electrons with energies larger than threshold (25):

$$\varepsilon_{b1} = N_\delta = 2C\varrho l \Delta^{1/2}. \tag{66}$$

The gas density ρ is proportional to Δ, so that we have in (64)

$$\varepsilon_{b1} \sim \Delta^{5/2},$$

and in the case of (66)

$$\varepsilon_{b1} \sim \Delta^{3/2}.$$

In the approximation considered, the efficiency of registering a particle by means of δ-electrons does not depend on the momentum of the particle.

To illustrate the quality of the approximation made, Fig. 7 shows two curves. Curve I is the probability for recording the particles with a threshold counter via the δ electrons, as a function of Δ, calculated by the approximate method developed above. Curve II is calculated more accurately, using graphic integration and a method analogous to that developed in Chapter III, with allowance for the path length and the deceleration of the δ-electron in the gas. Curve II has been calculated for the registration of a particle via δ-electrons near the threshold of its Cerenkov radiation in the given medium. Both curves pertain to a counter 70 cm long filled with ethylene. The product of the photomultiplier quantum sensitivity by the light gathering coefficient is assumed to be $\varepsilon\eta = 0.02$.

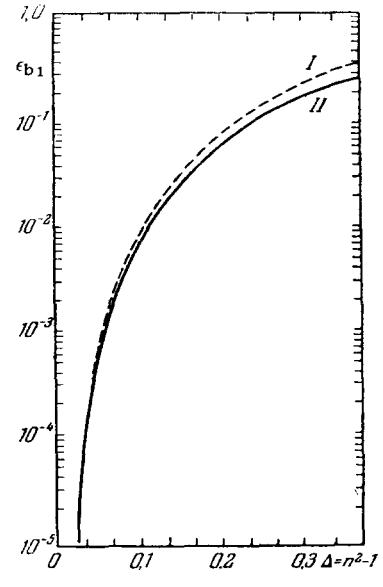

FIG. 7. Probability of registration of a particle in a TGC by means of δ-electrons, as a function of the refractive index of the gas. I—By formula (65); II—graphical integration.

It is seen from Fig. 7 that the approximate estimate agrees very well with the exact calculation in the region of small Δ and does not deviate much for large Δ. The approximate estimate is apparently sufficient for most practical cases of interest.

C2. The bremsstrahlung of heavy charged particles can be calculated by using [10]. If we make here several simplifying assumptions, namely: (1) we assume that the kinetic energy of the particle is

Table I. Energy lost by a particle to Cerenkov radiation (column 2) and to scintillation (column 3) relative to the ionization losses. Column 4—ratio of the scintillation losses to Cerenkov losses.

Gas	$10^3\cdot\left(\frac{dE}{dx}\right)_{Cer}/\left(\frac{dE}{dx}\right)_{ion}$	$10^3\cdot\left(\frac{dE}{dx}\right)_{sc}/\left(\frac{dE}{dx}\right)_{ion}$	$\left(\frac{dE}{dx}\right)_{sc}/\left(\frac{dE}{dx}\right)_{Cer}$
He	0.24	2.7	11
Ar	0.19	2.4	12.5
Air	0.27	$4\cdot10^{-3}$	$1.5\cdot10^{-2}$
N_2	0.28	2	7.1
Kr	0.14	5	36
Xe	0.14	8.7	62

large compared with the rust mass, (2) we neglect screening of the charge of the nucleus by the external electrons, and (3) we assume that the potential of the nucleus is the same as that of a point charge at distances larger than the nuclear radius r_n and is constant for distances smaller than r_n, where $r_n = 1.38 \times 10^{-13} A^{1/3}$cm, then we can readily obtain the number of photons radiated by the particle with mass m along a path of 1 g/cm^2 in the wavelength interval λ_1—λ_2:

$$N_b = 3^{-1}\alpha N A^{-1} Z^2 r_e^2\, 16 \left[\ln\left(\frac{\gamma^2\sqrt{\lambda_1\lambda_2}}{\pi r_n}\right) - \frac{1}{2}\right] \ln\frac{\lambda_1}{\lambda_2}.$$

Estimates show that for a pion with momentum ~ 5 BeV/c in the wavelength interval 6000—3000 Å we have $N_b = 1.2 \times 10^{-6}$ (Z = 6, A = 12). Since $N_b \sim 1/m^2$, for heavier particles this quantity will be even smaller and consequently the contribution of the bremsstrahlung to the formation of the TGC background can be neglected.

C3. Data relative to the scintillation of gases used in Cerenkov counters are practically nonexistent. We can therefore present only some general qualitative data.

The number of photons $I(\omega)$ emitted by the particle as the result of scintillations on a path length l in a frequency interval from ω to $\omega + d\omega$ is

$$I(\omega)\, d\omega\, dl = \frac{1}{\hbar\omega} B(\omega)\, d\omega \cdot \varrho \frac{dE}{dx} dl,$$

where $B(\omega)\,d\omega$ is the part of the particle energy going into radiation. The average number of photoelectrons produced on the photomultiplier cathode by the total light of the scintillation is determined by the equation

$$\overline{N} = \varrho \int_\omega \frac{1}{\hbar\omega} \varepsilon(\omega) B(\omega)\, d\omega \int_L \frac{dE}{dx} \eta(\theta, l)\, dl,$$

where $\varepsilon(\omega)$ is the quantum yield of the photomultiplier. We see therefore that $\overline{N}$ is proportional to the gas density. The proportionality coefficient depends on the nature of the gas and on the counter characteristics. Experiment has shown (see below) that the TGC efficiency below the Cerenkov radiation threshold is small, that is, the role of all the phenomena of the third group, including scintillations, is insignificant. Consequently $\overline{N} \ll 1$. On the basis of (52) we can assume that the TGC efficiency due to scintillations, ε_{b3}, is equal to $\overline{N}$ and is proportional to the gas density

$$\varepsilon_{b3} = \overline{N} \sim \varrho. \tag{67}$$

Naturally, when choosing a gas for Cerenkov counters, the scintillating ability of the gas must be taken into account. By way of illustration we can present data on the scintillations of inert gases and nitrogen, which is used in gas scintillation counters, and also air. The data on the relative light yield of scintillations of air are borrowed from [7].

Table I gives the particle energy losses to scintillation and Cerenkov radiation relative to the ionization losses. The Cerenkov losses are calculated for particles radiating light into the limiting angle.

From an examination of Table I we see that the relative energy losses to scintillation in inert gases exceed the maximum losses to Cerenkov radiation. It must be noted, however, that small impurities of gases such as oxygen, hydrogen, carbon dioxide, carbon monoxide, and a few others greatly suppress the scintillation of the inert gases and nitrogen[17].

D. Velocity Resolution of TGC

As was shown above, the efficiency of a threshold counter at a given refractive index is determined by the average number of photoelectrons (52). Let ε_1 and ε_0 be respectively the efficiencies of the counters for particles with velocities β_1 and β_0. It is obvious that the ratio $\varepsilon_1/\varepsilon_0$ will be maximal at a value of n corresponding to the radiation threshold for the velocity β_0, that is,

$$n = n_{t_0} = \frac{1}{\beta_0}. \tag{68}$$

The velocity resolution of the TGC can be defined as the difference of two velocities ($\Delta\beta = \beta_1 - \beta_0$), for which the average number of photoelectrons formed on the photomultiplier cathode varies from 0 to 1. This corresponds to a counter efficiency of 63%. Then, using (1), (49), and (68), we obtain

$$\overline{N} = 1 = A\left(1 - \frac{\beta_0^2}{\beta_1^2}\right),$$

hence

$$\frac{\Delta\beta}{\beta} = \frac{1}{2A}. \tag{69}$$

From (69) we can obtain the mass resolution of the TGC for particles having the same momentum, while the momentum resolution for particles having a definite mass

$$\frac{\Delta m}{m} = \frac{\Delta k}{k} = \frac{n_{t_0}^2 k^2}{2Am^2} . \quad (70)$$

We see therefore that the resolution of the TGC deteriorates with the increasing particle energy. Formulas (69) and (70) show also that the larger A, that is, the smaller the fraction of the radiated light is gathered by the optical system of the counter on the photocathode, and the larger the quantum yield of the photomultiplier employed, the better the resolution obtainable with the aid of the TGC.

III. OPTICS OF GAS-FILLED CERENKOV COUNTERS

The Cerenkov radiation of a particle moving parallel to the axis of a certain optical system is equivalent, as a light source, to a glowing ring located at infinity. If we use to gather the Cerenkov light a lens with focal distance f, then the linear diameter of the image of this ring at the focal plane is determined by

$$d_0 = 2f \operatorname{tg} \theta_0, \quad (71)$$

where θ_0 is the angle of Cerenkov radiation of a particle whose velocity is β_0. Particles of different velocity will produce a ring image with a different diameter. By placing an annular diaphragm in a suitable place, we can pass the light of the required particle and block the light from the remaining particles.

From the structural point of view, the most suitable is the case when the annular image of the registered particles is reduced to a point. To this end, as can be seen from (71), it is necessary to use a lens with a small focal distance. However, Marshall has pointed out [18] that for a counter of finite radius the quantity f cannot be made arbitrarily small and thus gather the Cerenkov light into ring of small diameter. The minimal focal distance, determined by law of conservation of the angular momentum of the photon relative to the optical axis of the system, is given by the expression

$$f_{\min} = rn \cos \theta_0,$$

where r is the radius of the counter radiator.

The requirements imposed on the optical system of threshold and differential counters are different. In a TGC the optical system must ensure the gathering by the photomultiplier cathode of the greater part of the Cerenkov radiation emitted by the particle, with the quality of the annular image being immaterial in first approximation. In the DGC, where good spatial separation of the annular image is necessary, produced by particles of different velocities, the requirements imposed on the optical system are quite stringent.

The quality of the image is determined by the aberrations of the optical system. The characteristics and the aberrations of the system depend to a considerable degree on the position and dimensions of the entrance pupil. We recall that the entrance pupil of an optical system is called the image of the aperture diaphragm in the object space.

The aperture diaphragm is the image in the object space of the same diaphragm of the optical system, the image of which is seen from the center of the object at the smallest angle.

Von Dardel [19] has shown that the entrance pupil of the optical system of a Cerenkov counter consisting of a radiator of length l and a lens is located in the center of the radiator, and has a diameter

$$D = d + l \operatorname{tg} \theta,$$

where d is the diameter of the particle beam. If the aperture of the objective is smaller than the cross section of the light beam incident on it, l must be taken to mean a certain effective length

$$l_{\text{eff}} = \frac{D_1}{2 \operatorname{tg} \theta} ,$$

where D_1 is the diameter of the aperture of the objective diaphragm. To improve the gathering of the Cerenkov light, it is possible to use a cylindrical reflecting tube, the axis of which coincides with the axis of the optical system. In this case the input pupil is the end of the tube and its diameter is equal to the diameter of the tube.

Let us stop to discuss monochromatic aberrations of optical systems. In calculating centered systems we use the theory of third-order aberrations (see, for example, [20-22]). In real optical systems, the image of a point from object space has the form of a scattering figure of complicated structure. The dimensions and form of this figure are determined by five coefficients S_I, S_{II}, S_{III}, S_{IV}, and S_V, called the aberration coefficients. Usually one investigates the scattering figures under the assumption that only one of the coefficients is not equal to zero.

The coefficient S_I determines the so-called spherical aberration. In the presence of spherical aberration in the optical system, an image of a point from object space has the form of a symmetrical scattering circle, the radius ρ_I of which is determined by the expression

$$\rho_I = \frac{1}{2} S_I \left(\frac{D}{f}\right)^3 . \quad (72)$$

Coma-aberration, which is determined by the coefficient S_{II}, is produced when a broad inclined beam of rays leaving the object point outside the axis is asymmetrical relative to the principal ray of the beam. For the simplest case of meridional coma, that is, asymmetry of a beam of rays lying in the meridional plane (which is the plane passing through the object point and the optical axis), the image of the point has the form of a bright circle of small dimensions with gradually broadening tail of considerably smaller

brightness. The radial length of the tail of the coma is $3\rho_{II}$, and its maximum width is $2\rho_{II}$, where

$$\varrho_{II} = \frac{1}{4} S_{II} \left(\frac{D}{f}\right)^2 \omega, \tag{73}$$

and ω is the angle of inclination of the light beam to the optical axis.

Astigmatism and curvature-of-field aberrations are determined by the coefficients S_{III} and S_{IV}, each of which is connected with the curvature of the focal surface in the meridional and sagittal planes (which is perpendicular to the meridional plane and crosses it along a line passing through the object point and the center of the system). If the focal surfaces in the meridional and sagittal planes do not coincide, the image of a point from the object plane has the form of an ellipse, the axes a and b of which are given by the formulas

$$4a = (S_{IV} - S_{III}) \left(\frac{D}{f}\right) \omega^2,$$

$$4b = (S_{IV} + S_{III}) \left(\frac{D}{f}\right) \omega^2. \tag{74}$$

The magnitude of the astigmatism is characterized by the difference

$$2a - 2b = -S_{III} \left(\frac{D}{f}\right) \omega^2. \tag{75}$$

If there is no astigmatism, that is, 2a − 2b = 0, then the image of the point will have, as a result of the curvature of the focal plane, the form of a scattering circle with radius ρ_{IV}, where

$$\varrho_{IV} = \frac{1}{4} S_{IV} \left(\frac{D}{f}\right) \omega^2. \tag{76}$$

The last of the monochromatic aberrations, distortion, causes the image of a point from object space to also have the form of a point, but at a position different from that given by an ideal optical system. The shift Δl of the image of the point from the position expected in accordance with Gaussian optics is proportional to the cube of the angle of inclination of the beam:

$$\Delta l = S_V \omega^3. \tag{77}$$

In real optical systems, individual types of third-order monochromatic aberrations are rarely encountered in pure form. In practice one observes a combination of aberrations of several forms, on which are superimposed aberrations of higher orders. Usually the design of an optical system is based on third-order aberration theory. The effect of higher-order aberrations is taken into account on the basis of an exact trigonometric calculation of the path of the rays through the optical system with subsequent subtraction of the third-order aberrations. For optical systems of Cerenkov counters it is possible to confine oneself in many cases to the calculation of the third-order aberrations.

It is necessary to take into account here the fact that for Cerenkov radiation the distortion and the curvature of the field do not influence the quality of the annular image, since distortion does not broaden the annular image, but only changes its diameter, while the broadening of the annular image due to curvature of the field can be avoided by shifting the image plane away from the Gaussian plane.

Let us consider the monochromatic aberrations of single concave mirrors and single lenses, these being the most frequently encountered optical systems in Cerenkov counters.

For a centered mirror and object at infinity, the third-order aberration coefficients are given by the formula [22]

$$\left.\begin{aligned} S_I = -\frac{(1+b)}{4}, \quad S_{II} = -\frac{x(1+b)}{4} + \frac{1}{2}, \\ S_{III} = -\frac{x^2(1+b)}{4} + x - 1, \quad S_{IV} = 1, \\ S_V = -\frac{x^3(1+b)}{4} + \frac{3x^2}{2} - 2x, \end{aligned}\right\} \tag{78}$$

where b is the coefficient of deformation of the surface (for a parabolic surface b = −1, for a spherical surface b = 0), and x is the distance from the input pupil to the top of the mirror.

It is seen from these formulas that the parabolic mirror, unlike the spherical mirror, does not have spherical aberration. Nonetheless, the mirrors usually employed are spherical, since the technology of their manufacture is much simpler than that of parabolic mirrors. For the case when the input pupil coincides with the top of the mirror, the formulas for the aberration coefficients of a spherical mirror have the very simple form

$$\left.\begin{aligned} S_I = -\frac{1}{4}, \quad S_{II} = \frac{1}{2}, \quad S_{III} = -1, \\ S_{IV} = 1, \quad S_V = 0. \end{aligned}\right\} \tag{79}$$

Let us consider the aberrations of a positive thin lens. For an object located at infinity, maximum spherical aberration is produced by a doubly convex lens with a surface radius of curvature ratio 6 : 1 and turned with the more convex side to the object. In practice, almost the same spherical aberration will be possessed by a planoconvex lens with its convex surface facing the object. For an object situated at infinity, and for an input pupil coinciding with the lens itself, the aberration coefficients of a planoconvex lens have the following value [22]

$$\left.\begin{aligned} S_I = 2.14, \quad S_{II} = -0.3, \quad S_{III} = 1, \\ S_{IV} = 0.6 \div 0.7, \quad S_V = 0. \end{aligned}\right\} \tag{80}$$

From a comparison with the aberration coefficients of a spherical mirror (79) we can readily see that for the same relative aperture (D/f) the spherical aberration of the lens is more than eight times

larger than the spherical aberration of the mirror, whereas the coma, astigmatism, and the curvature of the surface are practically the same for the mirror and for the lens. It therefore appears that for Cerenkov counters with high velocity resolution it is advantageous to use spherical mirrors and not lenses. The main advantage of mirrors is the absence of chromatic aberration. The chromatic aberration of a thin lens is given by the expression

$$\varrho_{\lambda_1\lambda_2}=\frac{D}{4f\nu_{\lambda_0}}. \tag{81}$$

Here λ_1 and λ_2 are the limits of the spectral intervals transmitted by the optical system and λ_0 is the wavelength corresponding to the maximum transmission of the optical system, with ν_{λ_0} the coefficient of dispersion:

$$\nu_{\lambda_0}=\frac{n(\lambda_0)-1}{n(\lambda_1)-n(\lambda_2)}.$$

Complex lens systems make it possible to compensate to some degree for the dispersion of the Cerenkov radiation.

For an estimate of the broadening of the maximum of the intensity curve of the Cerenkov light, we can assume that all the errors of the optical system are additive:

$$\varrho=\sum_{i=1}^{v}\varrho_i. \tag{82}$$

Then the angular width of the annular image of the Cerenkov radiation will be determined by the equation

$$\Delta\theta_{32}\approx\frac{\varrho}{f}, \tag{83}$$

where f is the focal distance of the optical system.

IV. GASES USED IN CERENKOV COUNTERS

A. Over-all Requirements and Attainment of Prescribed Refractive Index Intervals

In gaseous media it is possible to obtain in theory refractive indices with a wide range, from unity to quantities characteristic of liquids, but the practical realization entails great technical difficulties.

Most frequently there is no need for covering a large refractive-index interval in specific problems, so that it is possible to employ in the counters various gases that satisfy in best fashion the conditions of the particular experiment. All, however, should satisfy some general requirements.

The main characteristic of the DGC is the velocity resolution, determined by Eq. (5), from which it is seen that in order to obtain the best resolution for a given angle θ_0, that is, for a given n, it is necessary to choose a gas such that $\Delta\theta$ is minimal. From (11) and (15) (where $\Delta k_2 \sim \rho$) we see that $\Delta\theta$ increases with increasing density for a given refractive index. Consequently, it is necessary to choose the gas with the minimum $\rho/(n-1)$ ratio.

In addition to the velocity resolution, an important characteristic of DGC and TGC is the background, due essentially to the production of δ-electrons. Since their number increases, for a given refractive index, with increasing $Z\rho/A$ [see (29) and (65)], the most suitable gas has the smallest ratio $Z\rho/A(n-1)$.

One of the methods of obtaining different intervals of refractive indices is the variation of the gas pressure at constant temperature. The use of high pressures necessitates that the walls of the counter be sufficiently thick. This leads to an additional deterioration of the resolution and to an increase in the background of the counter. It is therefore necessary to choose a gas in which it is possible to obtain a given refractive index at lowest pressure.

On the basis of the foregoing considerations, a large number of gases was considered, of which the most suitable for the use in Cerenkov counters are listed in Table II.

In compiling Table II, the density was determined in most cases from the experimental data on the compressibility of gases, taken from the sources indicated in the last column. For some gases, in view of the lack of experimental data, the density was determined from the curves showing the dependence of the compressibility coefficient on the reduced pressures and temperatures (see [45,48]). For tentative calculations, Table II gives the values of the refractive indices of several gases at 20°C and at 50 atm. It is seen from the table that under such conditions it is possible to obtain a value of n in the interval from 1.01 to 1.06.

In order to vary n in the interval n = 1.1—1.2 at not too high pressures, it is necessary to employ gases at temperatures and pressures that are close to critical. The latter statement can be obtained from the following consideration [11]. We write the Lorentz-Lorenz formula in the form

$$\frac{n^2-1}{n^2+2}=\frac{4\pi}{3}N_1a,$$

where N_1—number of molecules in 1 cm^3 and a—optical polarizability of the molecules. It is known that a has the same order of magnitude as r^3—the cube of the linear dimensions of the molecule. If we assume that $a = r^3$, then at the critical point, where

$$\varrho_{cr}^{*}=\frac{1}{v_k}=\frac{M}{3b}$$

(b is the volume correction to the Van der Waals equation, equal according to kinetic energy to $4\pi Nr^3/3^3$, where N is the Avogadro number), we obtain

$$\frac{n_{cr}^2-1}{n_{cr}^2+2}=\frac{1}{12},$$

or $n_{cr} \approx 1.13$—the refractive index of any substance at the critical point. Of all the gases listed in Table II, ethylene at 20°C and at 50 atm comes closest to the critical point, so that it has the maximum refractive index.

Table II. Gases for Cerenkov counters and their characteristics

Gas	Chemical formula	T_{cr}, °C	P_{cr}, kg/cm²	$(n_D-1)\cdot 10^4$ (760 mm Hg, 0° C)	$(n-1)/\rho$, cm³/g	$\frac{A}{Z}\frac{n-1}{\rho}$, cm³/g	$(n_D-1)\cdot 10^2$ (20° C, 50 atm)	Literature
Hydrogen	H_2	—240	13.2	1.39	1.55	1.55	0.628	[44], p. 52
Oxygen	O_2	—118	51.7	2.72	0.143	0.286	1.26	[41], " 54
Air				2.926	0.226		1.35	[49], " 37
Nitrogen	N_2	—147	34.6	2.97	0.239	0.478	1.39	[44], " 50
Nitric oxide	NO_2	—93	66.1	3.03	0.226	0.452	1.50	[48], " 217—218
Carbon monoxide	CO	—140	35.6	3.34	0.269	0.538	1.54	[49], " 33
Ammonia	NH_3	132	115	3.77	0.488	0.832	0.328 *), 8.46 kg/cm²	[44], " 39
Methane	CH_4	—82.1	47.3	4.41	0.614	0.983	2.29	[50]
Carbon dioxide	CO_2	31.0	75.3	4.50	0.228	0.456	3.08	[49], p. 40
Freon-14	CF_4	—45.5	38.1	4.61	0.117	0.246	2.40	[49], " 70
Nitrous oxide	N_2O	36.5	74.1	5.15	0.260	0.520	4.11 *), 49.4 atm	[48], " 217—218
Acetylene	C_2H_2	35.7	63.7	6.10	0.521	0.965	4.80 *), 43.3 "	[44], " 32
Hydrogen sulfide	H_2S	100	91.8	6.19	0.402	0.760	1.36 *), 18.4 kg/cm²	[45], " 37
Sulfur dioxide	SO_2	158	80.4	6.60	0.225	0.450	0.221 *), 3.37 "	[44], " 62
Ethylene	C_2H_4	9.2	51.6	6.96	0.551	0.964	6.03	[44], " 59
Ethane	C_2H_6	32.3	49.8	7.06	0.521	0.866	4.56 *), 38.5 "	[51], " 62
Freon-13	$CClF_3$	28.8	39.4	7.82**)	0.156	0.326	4.00 *), 32.4 "	[51], " 55
Sulfur hexafluoride	SF_6			7.85	0.120	0.251		[49], " 68
Propane	C_3H_8	96.8	43.4	10.05	0.503	0.850	0.897 *), 8.50 "	[51], " 61
Freon-12	CCl_2F_2	112	40.9	11.27*)	0.204	0.422	0.646 *), 5.79 "	[51], " 49
Freon C-318	C_4F_8	115	27.6	12.85**)	0.144	0.300		[13]
Chloroform	$CHCl_3$	263	55.8	14.55	0.276	0.563		[13]
FC-75	C_8OF_{16}	221	16.3	27.4**)	0.148	0.308		

*At the saturated vapor pressure indicated alongside.
**Obtained by calculation based on molecular refraction[11,13].

B. Determination of the Refractive Index of a Gas

We have seen that gas Cerenkov counters make it possible to determine under suitable conditions the velocity [see (5)], the momentum [see (43)] and the mass [see (44)] of particles. To this end it is necessary to know exactly the refractive index of the gas, which can be measured experimentally or calculated by the Lorentz-Lorenz formula, if we know the molecular refraction and the density. For n close to unity, the approximate formula (7) holds, in which D does not depend on the density and its value for several gases can be readily obtained [23,24] from the known n – 1 and ρ, or can be calculated by using the additivity of the molecular refractions.

The gas density is determined experimentally or calculated with the aid of the equations of state. Most gases used in Cerenkov counters differ greatly from ideal. The constants of the equations of state (Van der Waals, Beatty-Bridgman) can be found in [23,44-46].

The validity of the Lorentz-Lorenz formula for the calculation of the refractive indices of polyatomic gases is, generally speaking, not obvious. Consequently a comparison of n was made in [30] for freon and for sulfur hexafluoride, obtained by the interference method and calculated by Eq. (6). It is seen from Figs. 8a and b that the agreement between the results is satisfactory.

On the basis of (5), (43), and (44) we can estimate that for an exact determination of the velocity, momentum, or mass it is necessary to know the refractive index with an error $\Delta n/n \leq 10^{-4}$. In view of the lack of exact data on the compressibility of gases and on their molecular refractions, it is practically impossible to ensure such accuracy by computation.

There are two methods of measuring the refractive index of a gas: with the aid of an interferometer and by determining the dielectric constant of a gas with a capacitor. We shall not consider the first method, referring those interested to the original sources [55-60]. The idea of the second method consists in the following. The formula for capacitance in a medium is

$$C = \varepsilon C_0, \tag{84}$$

where ε is the dielectric constant of the medium and C_0 is the rating of the given capacitor in vacuum (where $\varepsilon = 1$). For two wavelengths λ_1 and λ_2, corresponding to radio frequencies and to the visible region of the spectrum, we can write

$$\frac{\varepsilon(\lambda_1)-1}{\varepsilon(\lambda_1)+2} = A\rho, \quad \frac{n^2(\lambda_2)-1}{n^2(\lambda_2)+2} = B\rho,$$

where A and B are constants that do not depend on the wavelength or the gas density. Dividing one equation by the other and putting A/B = G, we get

$$n^2 - 1 = 3\left(G\frac{\varepsilon+2}{\varepsilon-1} - 1\right)^{-1},$$

from which we have, with account of (84),

$$n - 1 = \frac{3}{2G}\frac{C-C_0}{C+2C_0}. \tag{85}$$

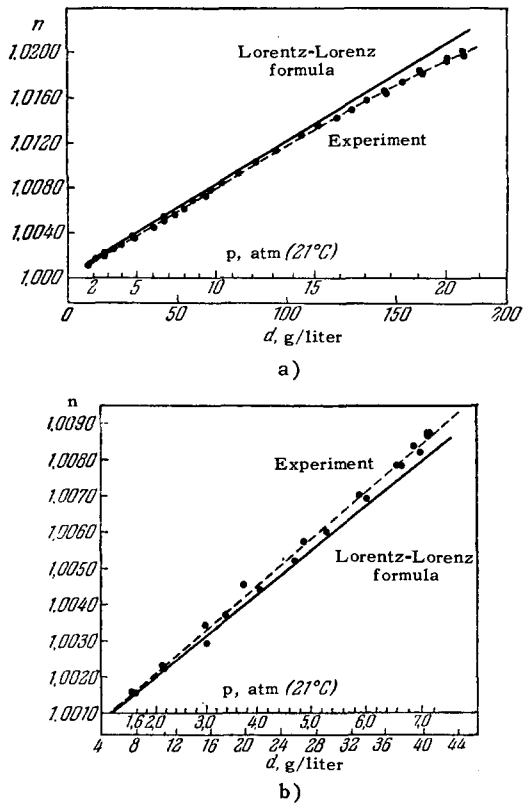

FIG. 8. Comparison of the refractive indices obtained by an interferometer method with that calculated by the Lorentz-Lorenz formula: a) For SF_6; b) for CCl_2F_2. The measurements were made for the wavelength 5400 Å. Abscissas–pressure (atmospheres), second scale–density (g/l).

Formula (85) is used to monitor the variation of n as a function of the gas pressure. The constant G can be determined if the refractive index and the values of the capacitances at one point are known.

If the capacitance is accurate to 10^{-3} pF [47], then for $n \approx 1.01$ and $C_0 \sim 100$ pF the error in the determination of the refractive index will not exceed $\Delta n/(n-1) \approx 7 \times 10^{-4}$ provided the constant G is known accurately.

C. Dispersion of Gases

Absolute measurements of the refractive index of many gases entail great difficulties in the elimination of various impurities. Consequently relative measurements are usually made, in which the refractive indices are compared for all wavelengths with some standard values $n(\lambda_0)$. The latter is determined beforehand by averaging of a series of measurements wherein the entire procedure, starting with the production of the gas, is duplicated. Although the relative variation of the dispersion is measured with high accuracy, the error in the absolute values of n is not smaller than for the standard value.

The variation of $n(\lambda)$ in the visible and ultraviolet regions has been obtained by the interference method in [55-60] for many gases used in Cerenkov counters. In these measurements n was compared with the refractive index $\lambda = 5461$ Å and reduced to 0°C and 750 mm Hg. The experimental dependence was approximated by formulas containing two constants:

$$\frac{1}{y} \equiv \frac{3}{2}\frac{n^2-1}{n^2+2} = A + \frac{B}{\lambda^2},$$

or four constants

$$\frac{1}{y} \equiv \frac{3}{2}\frac{n^2-1}{n^2+2} = \frac{A_1}{B_1-\lambda^{-2}} + \frac{A_2}{B_2-\lambda^{-2}}. \qquad (86)$$

In Table III are given the values of the constants of formula (86). As can be seen from the next to the last column, the accuracy of approximation, characterized by the quantity

$$\frac{y_{\text{theor}} - y_{\text{expt max}}}{y_{\text{expt}}} \cdot 100\%,$$

is of the order of 0.01.

Using the data of Table III we can show that dispersion of the refractive index in the wavelength region 2500–5500 Å causes the velocity resolution of the differential Cerenkov counters to be $\Delta\beta/\beta \sim 10^{-4}$–$10^{-5}$ for all the gases under consideration.

V. CONSTRUCTION OF GAS FILLED CERENKOV COUNTERS

A. Threshold Gas Counters

The first gas filled Cerenkov counters were of the threshold type. Following Ascoli and Balzanelly [5,6] and Barclay and Jelley [7], who worked with TGC at atmospheric pressure, counters were constructed with adjustable threshold of particle registration by velocity.

Tollestrup and Wentzel [25] described a counter used as a monitor for high-energy gamma quanta. The counter consisted of a tube 1 meter long, covered on the ends with thin flanges and filled with helium at low pressure. A converter was placed in front of the counter. The electrons produced in the converter emitted in the gas Cerenkov light which was deflected at the end of the tube by a plane mirror to a type 5819 photomultiplier. The monitor did not register individual pulses; the intensity of the beam was determined from the current in the photomultiplier cathode.

Kinsey and Wentzel [26] used a gas counter as a threshold detector for pions with energy ~3 BeV. The counter was made in the form of a tube with a parabolic mirror on the end, and the focus of which was located a 1P21 photomultiplier. The tube was filled with nitrogen at a pressure of several atmospheres. The gas counter connected in a triple-coincidence circuit with scintillation counters had a counting efficiency close to 100% for pions with energy 500 MeV above threshold.

Lindenbaum and Yuan [27] have reported the construction of a counter operating with carbon dioxide

Table III. Values of the constants in the gas dispersion formulas

Gas	Chemical formula	A_1	A_2	B_1	B_2	Region of application, Å	Accuracy, %	Literature
a) $\frac{1}{y} \equiv \frac{3}{2}\frac{n^2-1}{n^2+2} = \frac{A_1 \cdot 10^{-7}}{B_1 - 10^8\lambda^{-2}} + \frac{A_2 \cdot 10^{-7}}{B_2 - 10^8\lambda^{-2}}$ (λ in Å)								
Methane	CH_4	55813	626028	64.2208	181.2638	2300—5800	0.01	55
Ethane	C_2H_6	200355	1229245	72.2582	259.6137	2300—5800	0.01	55
Ethylene	C_2H_4	63682	851205	38.8407	158.7771	2300—5800	0.01	55
Propane	C_3H_8	437475	2577230	77.7600	504.7311	2300—5800	0.01	55
Ammonia		8656.0	442413.8	25.8837	131.2110	2300—5460	0.02	56
Dry air		571119.0	8700.3	211.146	49.5608	2379—5462	0.01	57
Carbon dioxide	CO_2	742030.0	4852.0	172.409	45.0378	2379—5462	0.01	58
Carbon monoxide	CO	49573.7	630960.0	549.894	266.076	2379—5462	0.01	58
Nitrogen oxide	NO	3482.94	485547.0	26.9925	176.1095	2300—5460	0.02	59
Nitrogen dioxide	NO_2	39454.3	750084.0	51.6712	179.3242	2300—5460	0.02	59
b) $\frac{1}{y} \equiv \frac{3}{2}\frac{n^2-1}{n^2+2} = \frac{A_1 \cdot 10^{-8}}{B_1 - 10^8\lambda^{-2}} + \frac{A_2 \cdot 10^{-8}}{B_2 - 10^8\lambda^{-2}}$ (λ in cm)								
Hydrogen	H_2	1428582	754494	116.3126	568.6707	2300—5460	0.01	57
Nitrogen	N_2	3953450	837340	152.294	240.651	2300—5460	0.01	60

at a pressure of 100-200 atm. Hanson and Moor [28] and Beneventano et al [29] used gas counters (T_1 and T_2), the construction of which is shown in Figs. 9 and 10, for the registration of cosmic muons. Both counters operated with compressed CO_2 at ~10 atm. They were triggered by a telescope of scintillation and Geiger counters and had efficiencies ~86 and ~97%, respectively.

Among the counters which were sort of "pioneers" in this field, we can also include the threshold gas counter (T_3) described by Belyakov et al [14], and which was used to investigate the possibility of obtaining high registration efficiency for particles and neat separation of rare particles against a large background of others. Its construction is shown in Fig.

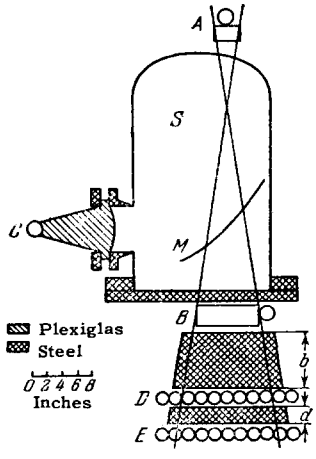

FIG. 9. The counter of Hanson and Moor. A, B, D, E—Telescopic counters, M—parabolic mirror; C—photomultiplier.

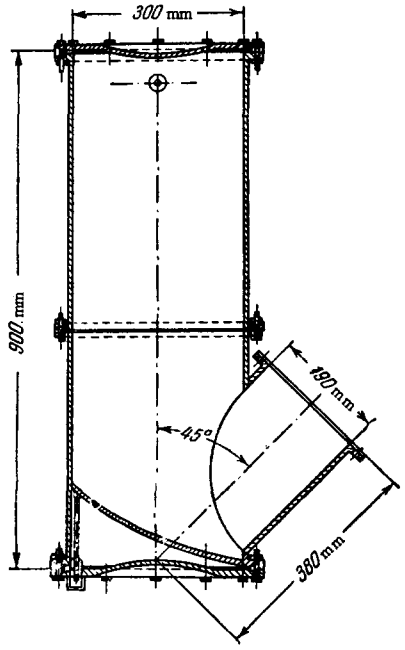

FIG. 10. Gas filled Cerenkov counter for the registration of cosmic muons.

11a. The steel tube and the flanges of the counters were designed for a pressure of 300 atm. Figure 11b shows the efficiency of the counter against the ethylene pressure, obtained with a 393-Mev pion beam. The curve shows clearly the presence of two plateaus, corresponding to the count of muons and pions. Analogous curves were obtained when the counter was filled with air. It is interesting to note that the background of the counter below the radiation threshold was approximately four times higher when filled with

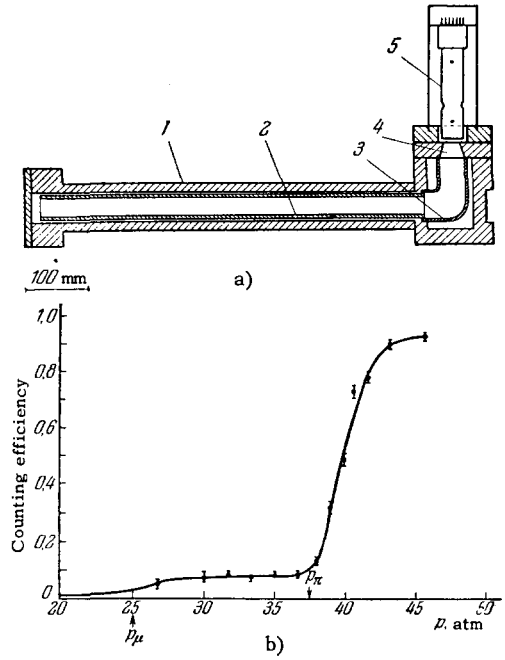

FIG. 11. TGC designed for 300 atm (T_3). a) Counter diagram: 1–steel housing, 2–aluminized glass tube 3 cm in diameter; 3–aluminized glass light pipe; 4–Plexiglas window; 5–FÉU-33 photomultiplier. b) Efficiency of counter T_3 as a function of the ethylene pressure. The curve was obtained in a 393-MeV π^+-meson beam. p_μ, p_π–threshold pressures for muons and pions, respectively.

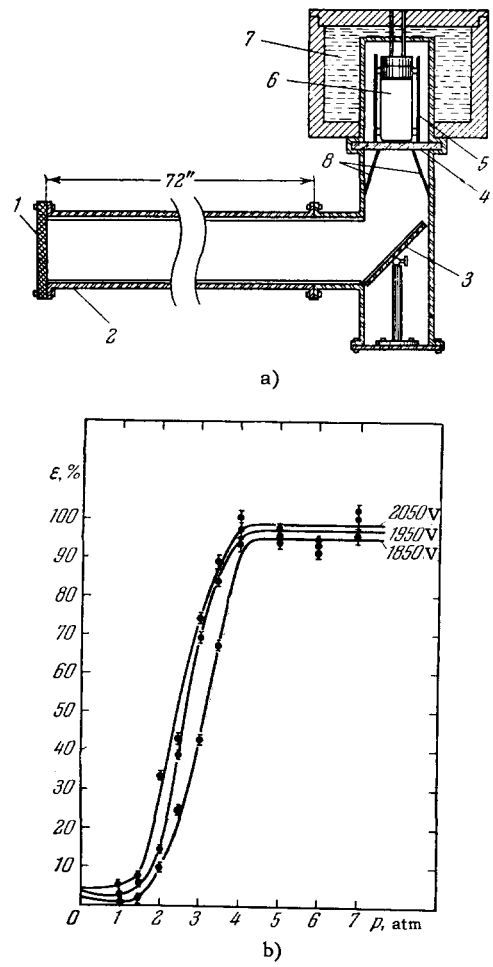

FIG. 12. a) Diagram of counter T_4: 1–aluminum flange 1.9 cm thick; 2–polished aluminum reflector; 3–flat aluminum mirror; 4–lucite window 1.9 cm thick; 5–magnetic screen of photomultiplier; 6–C-7232A photomultiplier; 7–dry ice; 8–polished aluminum cone. b) Efficiency of T_4 as a function of the SF_6 pressure at different photomultiplier voltages, measured in a beam of 3.0 BeV/c pions.

air than with ethylene. The densities of these gases have the same ratio. The magnitude of the background itself ($\sim$0.5%) is apparently due essentially to δ-electrons, since rotation of the counter through 180° reduced its efficiency to the level of random coincidences (0.1%), that is, the scintillations of the gas make a small contribution to the background.

Experience with the foregoing counters has shown that once their construction is improved, threshold gas filled Cerenkov counters can be used successfully as high efficiency detectors for high-energy charged particles. Subsequent experiments have confirmed this. Figure 12a shows a TGC (T_4) used for many years as a pion detector for energies above 3 BeV [30]. The counter consists of a steel tube, inside of which is inserted a tube of polished aluminum, a plane mirror deflecting the light through 90°, a polished aluminum cone to improve the light collection, and a type RCA-C7232A photomultiplier.

To reduce the number of noise pulses, the photomultiplier was cooled with dry ice located in a foamplastic box outside the jacket of the photomultiplier.

Figure 12b shows the counter efficiency as a function of the gas pressure (SF_6), obtained with a beam of pions with momentum 3.0 ± 0.1 BeV/c. The variation of the type of the curves as a function of the photomultiplier voltage offers evidence that the recording apparatus has a threshold corresponding to knocking out more than one photoelectron from the photomultiplier cathode. The count below the threshold is apparently due to the small fraction of the electrons always present in the pion beam. The smooth bend of the efficiency curve near the threshold of radiation can be attributed to the momentum scatter of the particles and to the muon admixture in the beam.

Swanson and Masek [31], on the basis of the construction just discussed, produced a large TGC (T_5) for operation in a 2-BeV/c muon beam (Fig. 13a). The counter is 2.2 meters long and has a diameter of 32 cm. The difference from the construction in [30] lies in the fact that in order to improve the light gathering, a Fresnel lens of 30 cm diameter and 30 cm focal distance is used to focus the light on the RCA 7264 photomultiplier. The efficiency of the counter for 2 BeV/c muons and pions is shown in Fig. 13b as a function of the gas pressure (CO_2).

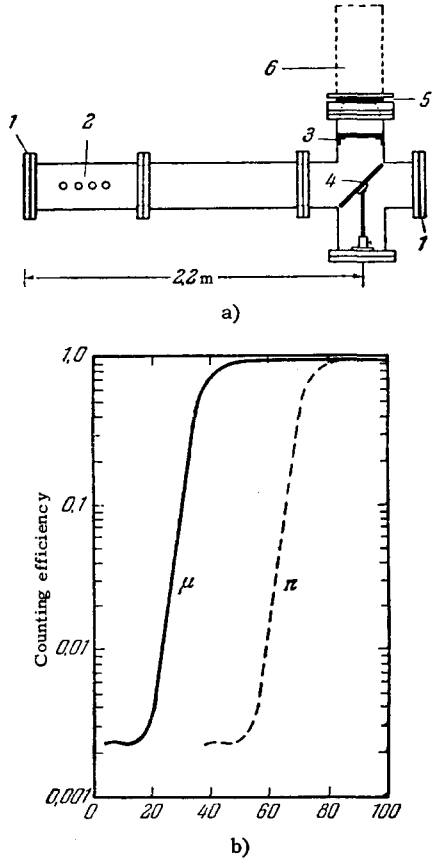

FIG. 13. a) Diagram of counter T_5: 1–thin aluminum window; 2–holes for gas and for pressure measurement; 3–Fresnel lens; 4–mirror; 5–lucite window; 6–photomultiplier in magnetic shield. b) Efficiency of counter to muons (solid curve) and pions (dashed curve) with momentum 2 BeV/c as a function of the CO_2 pressure. Abscissas–Counter pressure above atmospheric (in pounds per square inch).

Babaev and Landsberg [32] described the counter (T_6) shown in Fig. 14. This counter was tested with a beam of 200-MeV/c electrons and had an efficiency ~100% at a freon-13 pressure of 5 atm. When the counter was turned through 180°, its efficiency decreased to 1.4%.

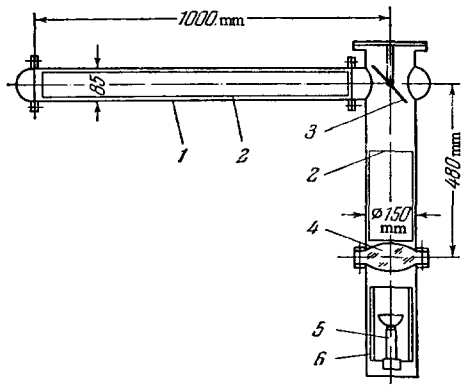

FIG. 14. Diagram of the counter T_6. 1–Housing of counter; 2–cylindrical mirror; 3–flat mirror; 4–lens; 5–FÉU-24 photomultiplier, 6–magnetic shield of photomultiplier.

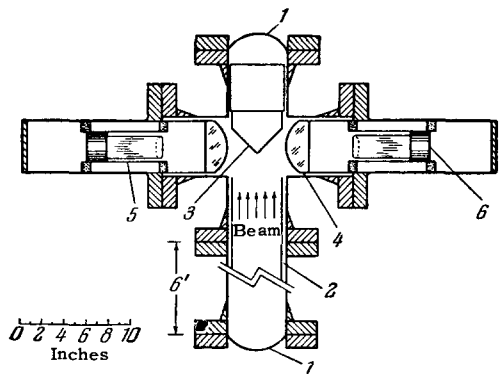

FIG. 15. Diagram of the counter of Cork et al [40]. 1–Aluminum windows 0.75 mm in diameter; 2–cylindrical mirror of anodized aluminum 15 cm in diameter; 3–flat mirror of anodized aluminum; 4–lucite lens 10 cm in diameter; 5–magnetic shield of photomultiplier; 6–6810-A photomultiplier.

The counter shown in Fig. 15 was used to measure the differential cross sections of elastic $\bar{p}p$ scattering [40]. It was connected for anticoincidence with other counters to suppress the pion background.

The gas threshold counters (T_7, T_8, T_9), shown in Fig. 16a, b, and c, respectively, were used in the high-energy laboratory of the Joint Institute for Nuclear Research.[14,53,54] A characteristic feature of these counters is the use of an inclined parabolic or

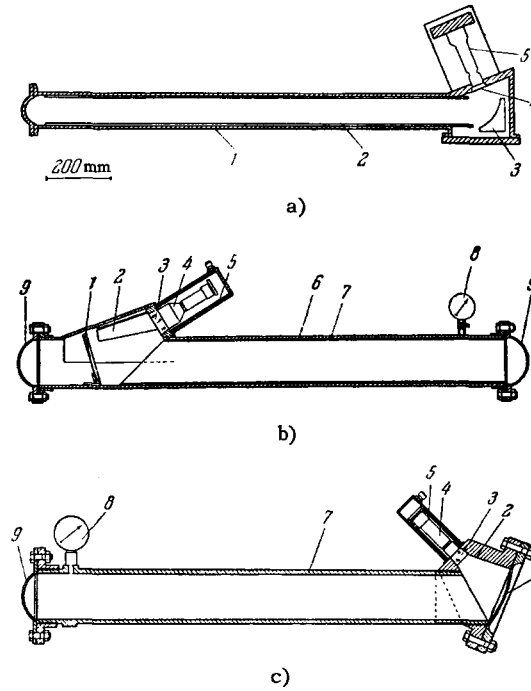

FIG. 16. a) Diagram of counter T_7: 1–steel tube 10 cm in diameter; 2–aluminum reflector; 3–parabolic mirror; 4–quartz window; 5–FÉU-33 photomultiplier. b–c) Diagrams of counters T_8 and T_9, respectively; 1–spherical mirror; 2–aluminized conical reflector; 3–Plexiglas window; 4–photomultiplier; 5–magnetic shield of photomultiplier; 6–polished aluminum tube; 7–tube (in counter T_8–steel, in counter T_9–duraluminum); 8–manometer; 9–flange.

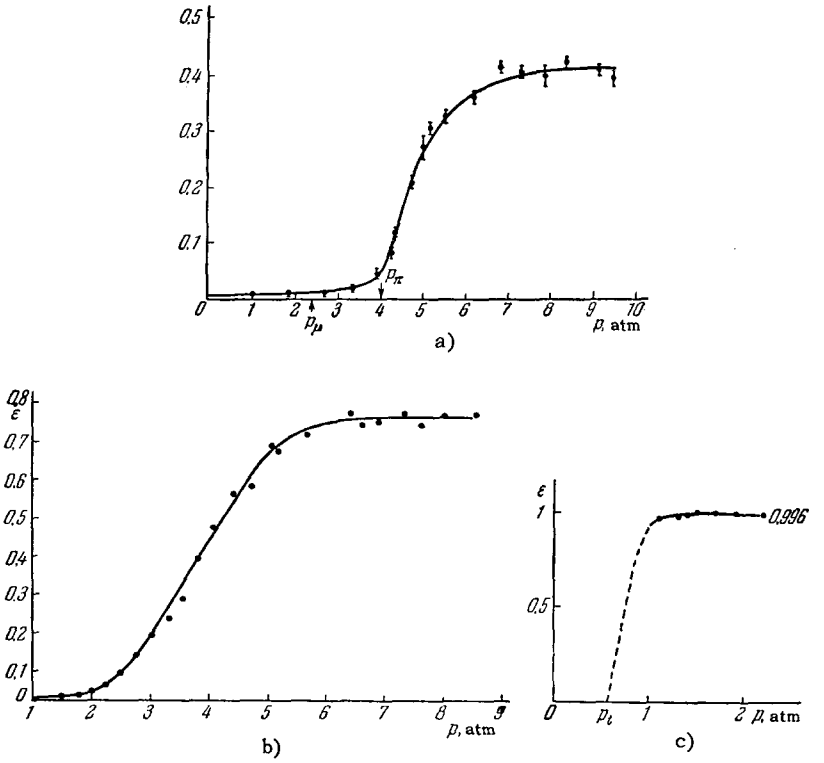

FIG. 17. a) Registration of negative pions with 2.95 BeV/c momentum with counter T_7, as a function of the air pressure. b) Registration of negative pions with momentum 3.9 BeV/c with counter T_8 as a function of the air pressure. c) Efficiency of counter T_9 for positive pions with momentum 4 BeV/c as a function of the pressure of the Freon-12. Dashed curve–extrapolation to the threshold pressure.

spherical mirror in order to bring the photomultiplier out of the particle beam. This circumstance greatly simplifies the construction of the counter and its manufacture. Data on tests of these counters are given in Fig. 17. All the counters operated with electronic apparatus having a sensitivity corresponding to the formation of 1 photoelectron on the photomultiplier cathode.

A giant threshold gas counter has been constructed at CERN [86]. It is 10 meters long, with an inside diameter 15 cm, and is intended for the separation of pions, muons, and electrons up to 10 BeV energy. The counter consists of a tube made up of individual 80 cm sections, at the end of which is secured a flat mirror, deflecting the light. The light is gathered on a type 56 UVP photomultiplier with the aid of a parabolic mirror. The working medium is hydrogen, which is the most convenient gas from the point of view of minimum production of δ-electrons, energy loss to ionization, and multiple scattering. Under ordinary conditions the gas pressure is set such as to make the glow angle equal to 1°. In this case a total of 140 photons is produced in the spectral region of the photomultiplier sensitivity. Tests have shown that when tuned for registration of the electrons the counter has a high efficiency (better than 99%) and a high degree of suppression of the heavier particles.

Let us consider the resolution of the described Cerenkov threshold counters. The form of the efficiency curve of the TGC near threshold of Cerenkov radiation is influenced by many various factors (admixture of muons in the electron beam, momentum scatter of these particles, sensitivity of the electronic apparatus), the contribution of which is difficult to evaluate. Therefore the determination of the threshold pressure and the use of formulas (69) and (70) for the calculation of the TGC velocity resolution, mass resolution, or momentum resolution is made very difficult. On going farther from the threshold, the effect of the foregoing influences becomes smoothed out and the slope of the efficiency curve is determined to an ever increasing degree by the constant A of the counter. It can be assumed that an efficiency of 10% all the near-threshold phenomena become already smoothed out. Consequently, as a characteristic of the resolution of a counter we can choose the section of the efficiency curve of the TGC, plotted against pressure, between the levels 10 and 90% [30]. Since the counter efficiency is a function of $\sin^2\theta$, it is obvious that the quantities

$$\left.\begin{aligned} c_1 &= 1 - \frac{1}{n_1^2\beta^2}, \\ c_2 &= 1 - \frac{1}{n_2^2\beta^2}. \end{aligned}\right\} \qquad (87)$$

where n_1 and n_2 are the refractive indices corresponding to the efficiencies 90 and 10%, will also be constants of the counter. To derive the momentum resolving power of the counter, we write c_1 and c_2 in the form

$$\left.\begin{aligned} c_1 &= 1 - \frac{1}{n^2\beta_1^2}, \\ c_2 &= 1 - \frac{1}{n^2\beta_2^2}. \end{aligned}\right\} \qquad (88)$$

From this we readily obtain the value of the momentum k_2, for which the counter has an efficiency 10% if it has an efficiency of 90% for k_1:

$$k_2 = \frac{m_1 k_1}{\sqrt{\frac{c_1 - c_2}{1 - c_1}(k_1^2 + m_1^2) + m_1^2}}. \quad (89)$$

It is interesting to know which pairs of particles can separate the counter in a beam with given momentum. From (88) we readily obtain the kinetic energy T_1 of a lighter particle m_1, registered by a counter with efficiency 90%, at which the heavier particle m_3 will be registered with efficiency of 10%:

$$T_1 = m_1 \left\{ \frac{1}{\sqrt{\frac{m_1^2}{m_2^2 - m_1^2}\frac{c_1 - c_2}{1 - c_1}}} - 1 \right\}. \quad (90)$$

Tables IV and V give respectively the momentum and mass resolutions of the discussed counters, calculated by formulas (89) and (90). An examination of these tables shows that the threshold counters have good momentum resolution up to approximately 1.5 BeV/c. At larger energies, the resolution deteriorates rapidly, in accordance with formula (70).

It is seen from Table V that the TGC are good devices for the separation of particles by masses in a beam with given momentum. Therefore, to separate the light particles, the gas pressure is set in such a way that the heavier particles are below the radiation threshold. The counter is connected for coincidence with scintillation counters which register both light and heavy particles. When separating heavy particles, the TGC is connected for anticoincidence with the scintillation counters.

The accuracy of separation of the lighter particle depends on the ratio of the counter background to the efficiency on the plateau. The curves obtained by testing the foregoing counters show that the lowest background obtained in ~ 0.002 of the efficiency at the plateau (counter T_5). Nothing definite can be said with respect to the background in the other counters, since they were tested under conditions in which the presence of high-energy electrons in the beam was not excluded. The background can be reduced by connecting two or more TGC for coincidence or by raising the sensitivity threshold of the electronic apparatus. The purity of separation of the heavy particles is determined by the efficiency of the counter at the plateau and by the efficiency of the anticoincidence circuit. The test curves of counters T_5 and T_6 show that the best experimentally obtained efficiency is 0.996. This means that if the electronic anticoincidence circuit has an efficiency of 100%, then it is possible to suppress with the aid of such TGC the lighter particles by a factor better than 250.

Table IV. Momentum resolution obtained with threshold Cerenkov counters

k(90%), BeV/c	$k_1 - k_2 = \Delta k$(90 ÷ 10%) MeV/c						
	T_4	T_7	T_3	T_9	T_8	T_6	T_5
4.0	1000	800	2600	510	930	1120	650
3.0	720	630	1700	470	700	800	550
2.0	260	230	900	170	250	1300	200
1.5	120	110	530	80	130	150	120
1.0	40	40	220	30	45	50	35
0.5	8	7	40	~1	10	10	8

Table V. Separation of different particle pairs by means of Cerenkov threshold counters. The table gives the kinetic energy of the lighter particle (in BeV), at which the heavier particle is counted with an efficiency of 10%

Counters	$\mu - \pi$	$\pi - K$	$K - p$	$\pi - p$
T_3	0.83	4.2	7.1	8,3
T_4	2.2	12	19	23
T_5	2.75	15	25.5	29
T_6	2.0	11	14.5	21
T_7	2.5	13.3	23.5	26
T_8	2.3	12	21	24
T_9	3.0	16	28	32

B. Differential Gas Counters

The family of differential counters is less numerous than the family of threshold counters. This is connected, first, with the fact that their construction began more recently; second, because they constitute rather complicated instruments with precision optics.

The first to be described was a DGC (D_1) in which the refractive indices of the medium could be varied over a wide range up to 1.277[13,39,33,35].

The working medium in the counter was the fluoro-organic compound perfluorotributyl tetrahydrofuran (C_8OF_{16}), the commercial designation of which is FC-75. At normal pressure and temperature this is a liquid with low critical pressure 16.3 atm and a critical temperature 227.1°C. Refractive indices of the order of 1.1—1.2 can be obtained in this substance at relatively low pressure, by heating it to ~ 250°C. A schematic diagram of the counter is shown in Fig. 18a. The housing of the counter, 25 cm long and 10 cm in diameter, is made of copper; the inside surface is polished and chrome plated. The exit window for the particle beam is a hemispherical steel membrane 1.6 mm thick. The exit window for the light is made of quartz 2.5 cm thick. The counter is heated by a heating element surrounding its housing. To reduce the temperature and the pressure, a larger or smaller amount of FC-75 is admitted into the working volume. A spare reservoir of liquid is kept at room temperature. The pressure in the system is varied by varying the pressure of the nitrogen

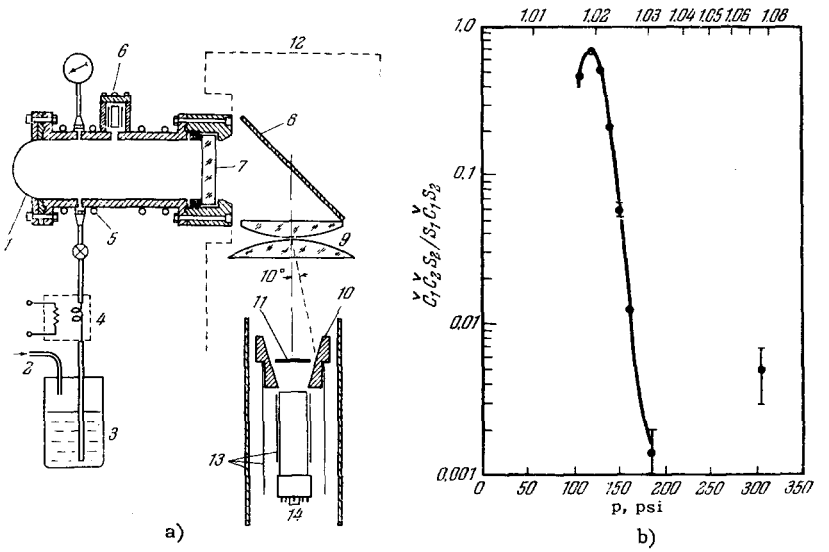

FIG. 18. a) Diagram showing construction of the counter D_1: 1–hemispherical steel entrance flange 1.6 mm thick; 2–nitrogen fed under pressure; 3–FC-75 liquid; 4–heater; 5–heating element; 6–capacitive density transmitter; 7–quartz window; 8–plane mirror; 9–quartz lenses; 10–conical reflector; 11–black disc; 12–light-tight box; 13–magnetic shield of photomultiplier; 14–C7267 photomultiplier, b) Efficiency of counter D_1 for pions with momentum 2.6 BeV/c. On the abscissas–the lower scale is the gas pressure (in pounds per square inch) and the upper scale is the refractive index.

over the liquid in the spare reservoir. In order for the liquid FC-75 flowing from the reservoir not to change the temperature of the medium in the counter, a thermostat-controlled heater is connected in the line to the instrument. The refractive index of the medium is monitored by means of a capacitive transducer.

The optical system of the counter is designed for registration of particles which radiate light at an angle $\sim 10°$ to the direction of motion. It consists of a deflecting plane mirror, a two-lens focusing element corrected for coma and astigmatism, but having small spherical and chromatic aberration, and a diaphragm made up of a black moving disc and an aluminized conical reflector. The calculated width of the annular image in the focal plane has dimensions of 1.08 mm or 0.3° due to spherical aberration and 3.1 mm or 0.8° due to chromatic aberration. The lenses are made of quartz and lucite. The Cerenkov light is registered with an RCA-C7267 photomultiplier with a quartz window.

Taking into account the spectral distribution of the intensity of the Cerenkov radiation, the transparency of the quartz, and the spectral sensitivity of the photomultiplier, it can be shown (see [1], page 127) that when a quartz optical system is used the number of photons reaching the surface of the photocathode of the photomultiplier is twice as large as when lucite or glass optics are used.

Figure 18b shows the dependence of the count in D_1 on the gas pressure, obtained in a positive pion beam with momentum 2.6 BeV/c. The diaphragm transmitted in this case light emitted at angles 9.5–10.5°. The efficiency of the counter at the maximum (68%) is a function of the threshold of the electronic apparatus. It can be increased, but the width of the maximum and the ratio of the background to the efficiency at the maximum increases accordingly.

The velocity resolution of the counter, calculated from the half width of the efficiency curve at half height, $\Delta\beta/\beta = \Delta h/h = 0.0025$, is close to the theoretical value 0.002 given by formula (7). The background in the counter is 0.0015 at a pressure of 14 atm. With further increase in the pressure, the background increases, apparently because of an increase in the number of δ-electrons.

Counters of the construction described were used in experiments on the study of the total cross sections of the interaction of π and K^+ mesons with protons [36,37]. Figure 19 shows an example of the separation of K^+ mesons from a beam of particles with momentum 2.6 BeV/c.

A large DGC(D_2), constructed at CERN [33,35,38] is designed to operate with ethylene up to a pressure of 70 atm* (Fig. 20). The refractive index limits are 1.0–1.15 at 22°C. A capacitive transmitter, calibrate with the aid of a refractometer, is provided for meas-

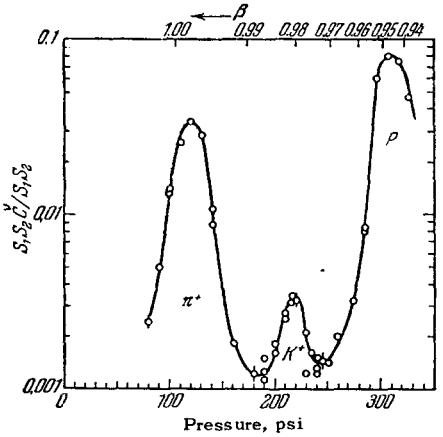

FIG. 19. Mass spectrum obtained with the aid of D_1 in a beam of particles with momentum 2.6 BeV/c. Abscissas–pressure in pounds per square inch.

*See [65] concerning the use of a counter of similar construction.

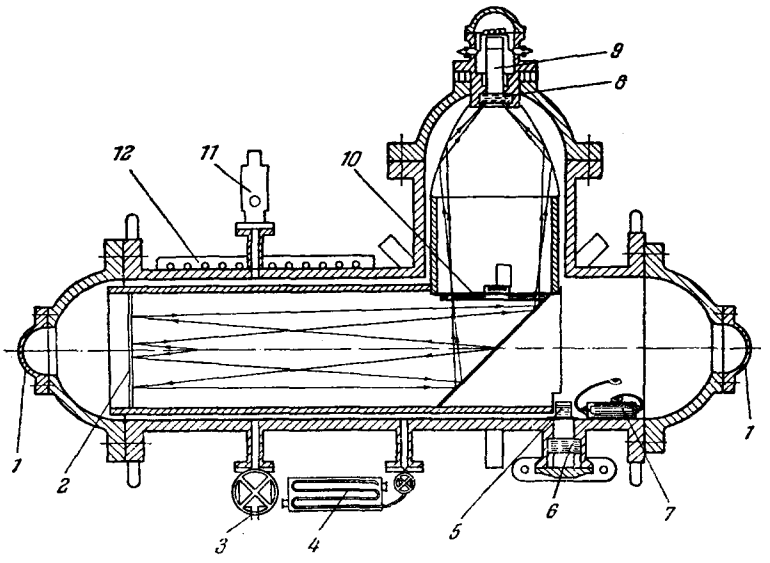

FIG. 20. Differential counter D_2. 1–Aluminum windows; 2–spherical mirror; 3–to vacuum pump; 4–gas inlet; 5–refractor prism; 6–window for observation; 7–capacitive transmitter; 8–quartz window; 9–photomultiplier; 10–variable annular diaphragm; 11–safety valve; 12–heating element.

urement of the refractive index in the counter. The gas temperature is maintained constant by water circulating around the counter and connected with a thermostat. The Cerenkov light is focused with a centered spherical mirror with large focal distance f = 130 cm and with small relative aperture (D/f), making it possible to obtain an annular image of high quality. The most important are the coma and astigmatism aberrations. For particles traveling at a distance of 8 cm from the optical axis of the mirror and emitting light at an angle 0.1 rad, the broadening of the ring due to coma and astigmatism is 0.6% of the radius of the annular image. The broadening of the ring due to dispersion of the refractive index in the region of the spectral sensitivity of the photomultiplier cathode is 1%.

To take the photomultiplier outside the particle beam, a plane mirror is used, which deflects the Cerenkov light onto an annular diaphragm. The diaphragm is located at the focus of the spherical mirror. It has a stationary central part, corresponding to a radiation angle of 0.1 rad, and a variable annular slot, the angular width of which can be regulated from 0 to 0.03 rad. Since according to (71) the given spherical mirror gives an annular image of 26 cm diameter, it is necessary to employ an additional optical system, in the form of an aluminized elliptical cone, in order to gather the light passing through the diaphragm onto the cathode of the photomultiplier.

Light strikes the photomultiplier through a quartz window 8 cm in diameter. The path length of the particles that radiate useful light (~500 photons) is 1 meter. The total length of the counter is 2.5 meters and the weight is 3 tons.

The theoretical resolution of the counter is shown in Fig. 21. An example of a velocity spectrum, determined with the aid of the given counter in a particle beam with momentum 18 BeV/c and with divergence of 1.7 mrad is shown in Fig. 22. The π, K, and p peaks are obtained with an annular diaphragm 2 mrad wide. The counter has then an efficiency of 72% and a velocity resolution $\Delta\beta/\beta = 3 \times 10^{-4}$. The deuteron peak has been measured with an annular diaphragm 6 mrad wide. The counter efficiency was then close to 100%. The background of the counter is $\sim 10^{-4}$.

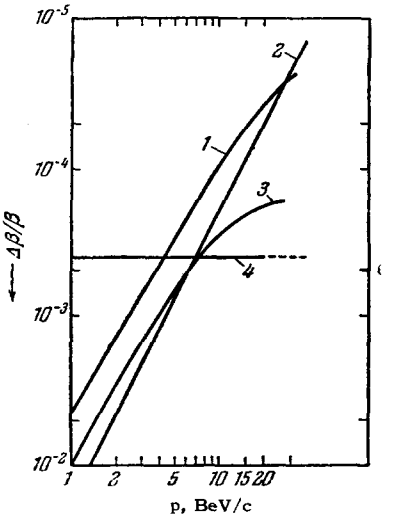

FIG. 21. Factors determining the theoretical velocity resolution of the counter D_2 as a function of the particle momentum. 1–Multiple scattering, 2–momentum scatter (15%), 3–dispersion (3%), 4–beam divergence (2×10^{-3} rad).

Cork et al [39] constructed a counter D_3, which operates simultaneously with two angle intervals. Figure 23a shows a section through this counter. The radiating volume of gas (methane) is in the form of a tube 12.7 cm in diameter and 70 cm long, covered with thin aluminum flanges ~5 mm thick. The Cerenkov light is deflected by 90° by a plane mirror and two side arms, which contain lucite lenses which

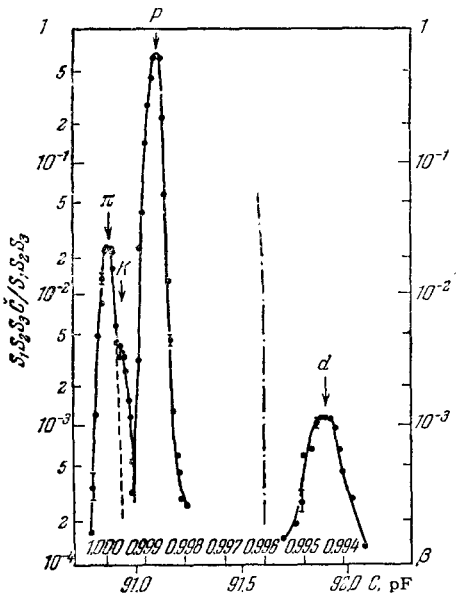

FIG. 22. Velocity spectrum of beam of positive 18 BeV/c particles, obtained with the aid of the counter D_2. The second scale on the abscissa axis—variation of the capacitance with variation of gas pressure in the counter.

focus the light into a ring on a quartz window. If the angular radius of the ring is smaller than 6.6°, then the light strikes a central photomultiplier through a conical light pipe. If the angular radius is larger than 7.4°, the light strikes four photomultipliers located on a ring and operating in parallel. The theoretical velocity resolution of the counter is $\Delta\beta/\beta = 2 \times 10^{-3}$.

Counter D_3 was intended for a special purpose—to separate K mesons with momenta from 1.5 to 5 BeV/c in a particle beam. It was operated in conjunction with a system that separated K mesons by time of flight. The operating circuit of the counter differed with the particle momentum: mode A—momentum larger than 1.5 BeV/c, mode B—smaller than 1.5 BeV/c. Mode A consists in the following. The pressure in the counter is chosen such that the K mesons produce a Cerenkov light at an angle 6°, which is gathered by the central photomultiplier. The Cerenkov radiation from the π, μ, and e particles is focused on the outer ring. The signals from the central photomultiplier are connected for coincidence with the scintillation counters, while the signals from the external photomultiplier are connected for anticoincidence. A typical curve illustrating the operation of the counter in this mode as a function of gas pressure is shown in Fig. 23b. The particle momentum is 2 BeV/c. At a pressure of 100 to 400 psi, the efficiency is close to unity and the counter registers π, μ, and e particles whose light reaches the central photomultiplier. With increasing pressure, the light shifts to the outer ring and the count decreases sharply, to a value $\sim 10^{-6}$. The K-meson glow

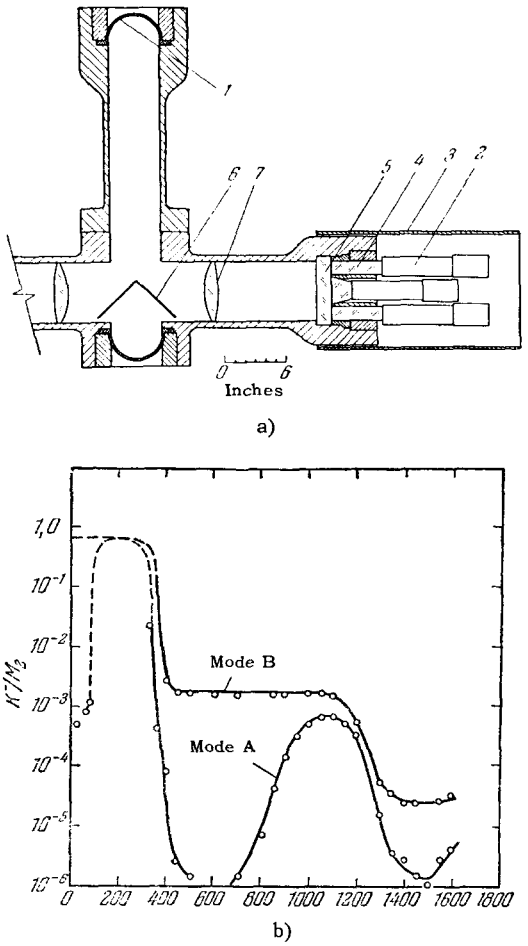

FIG. 23. a) Diagram of counter D_3: 1—aluminum hemispherical window ~ 5 mm; 2—6810 A photomultiplier; 3—magnetic shield of photomultiplier; 4—lucite light pipe; 5—quartz window ~ 3.8 cm; 6—plane aluminum mirror; 7—lucite lens. b) Efficiency curves for K mesons at different operating modes as a function of the methane pressure. Abscissas—pressure (in psi).

threshold is 700 psi, and the count due to these mesons reaches a maximum at ~ 1000 psi.

In mode B, the signal from the central photomultiplier is not necessary. The counter operates only for anticoincidence. So long as the Cerenkov light does not strike the outer ring, the apparatus counts the particles $\pi + k + p$ (first plateau on Fig. 23b). With increasing pressure, the particle glow angle increases, and light on the outer photomultiplier is produced first by the π mesons and then by the K mesons. Accordingly, the electronic apparatus counts $k + \tilde{p}$ particles (second plateau) and $\tilde{p}$ particles (third plateau).

An interesting example of the use of gas Cerenkov counters is described by Cook [41]. The counter, the construction of which is shown in Fig. 24a and b, was used in measurements of elastic K^-p scattering in anticoincidence, to exclude the secondary products of K meson decay, which distort the angular distribution

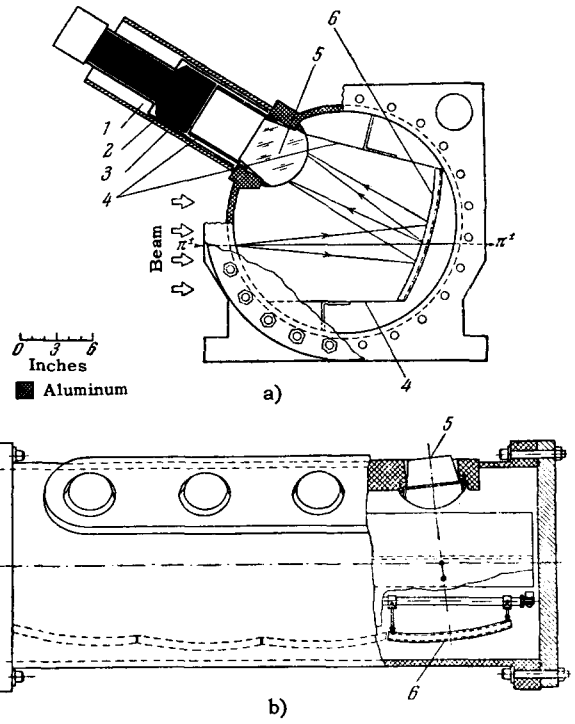

FIG. 24. Diagram of the counter of Cook et al. a) 1, 3–Magnetic shield of photomultiplier; 2–7046 photomultiplier; 4–anodized aluminum reflector; b) 5–lucite lens; 6–aluminized spherical mirror (~ 30 × 30 cm, radius of curvature ~ 71 cm).

of the scattered K mesons. The pressure of the gas (SF_6) was adjusted such that the particles with velocity $\beta = 1$ emitted light at an angle of 10°. The Cerenkov radiation was focused by a spherical mirror on a Plexiglas stopper, which simultaneously served as a lens.

Figure 25 shows the diagram of a DGC (D_4) developed and employed at the High-Energy Laboratory of the Joint Institute for Nuclear Research to separate K mesons [42,43]. The Cerenkov radiation is produced in a steel tube (10 cm diameter) filled with gas. The tube is closed on both sides with stainless steel flanges 1 mm thick. It was initially polished, but during the tests it was found that the counter background depends strongly on the quality of the polish. Therefore the internal surface of the counter was subsequently covered with black velvet, so as not to gather the reflected light. The counter length was 1.6 mm and the velvet coating decreased the effective length of the counter to 0.7 meters.

The optical system of the counter D_4, consisting of a spherical mirror with focal distance 40 cm, the axis of which is inclined to the axis of the particle beam, is set for registration of Cerenkov radiation emitted at an angle of 4°.

The use of an inclined mirror in place of a centered mirror has made it possible to remove the photo-

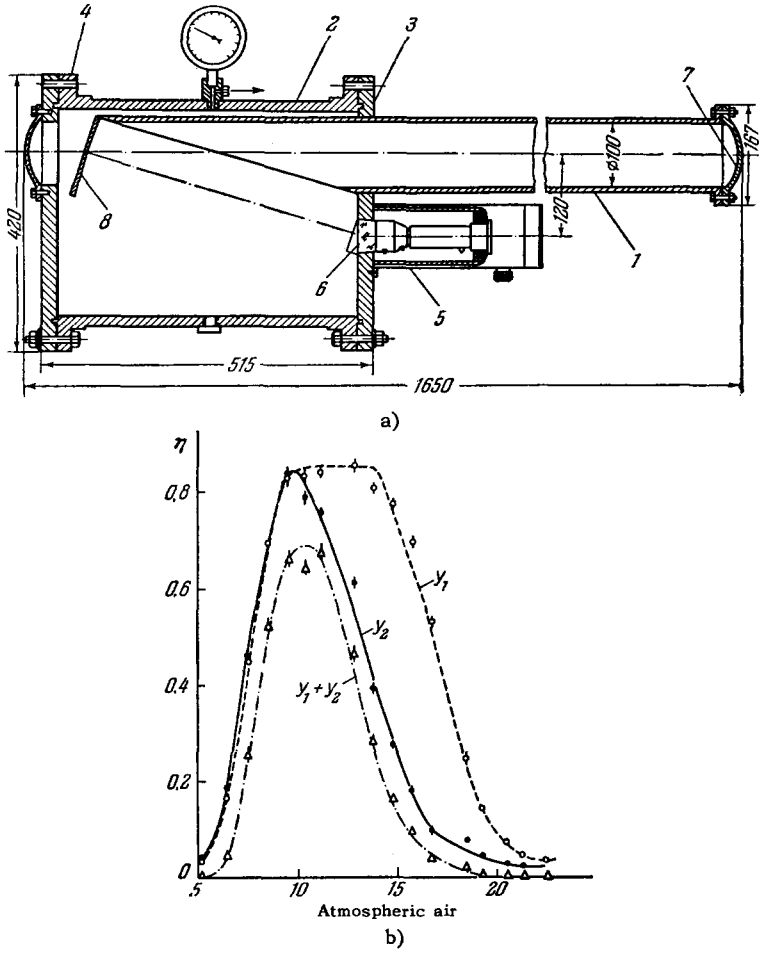

FIG. 25. a) Diagram of counter D_4 (dimensions in millimeters): 1–steel tube; 2–counter housing; 3, 4–removable flanges; 5–FÉU-24 photomultiplier; 6–Plexiglas window; 7–flanges of stainless steel, 1 mm; 8–spherical mirror (f = 40 cm). b) Efficiency of two counters D_4 to 3.4-BeV/c pions as a function of the air pressure: Y_1–10 mm diaphragm; Y_2–4 mm diaphragm, $Y_1 + Y_2$–both counters connected for coincidence.

multiplier from the particle beam without the use of additional plane mirrors. The aberrations of such a mirror can be estimated by regarding it as part of a larger mirror, the axis of which coincides with the radiator axis. It is clear that the aberrations of the part of the mirror will not exceed the aberrations of the entire surface. The calculations show that the most essential in this case is the spherical aberration, which amounts to 10% of the image radius.

Counting efficiency curves for two DGC of this type, with annular diaphragms 10 and 4 mm wide, plotted against the pressure of the air in them, are shown in Fig. 25b. The inside diameter of the diaphragms is the same. The curves were obtained in a π^+ meson beam with momentum 3.4 BeV/c. Since few photons are produced in the counter (~ 150), in order to obtain high counting efficiency it is necessary to select carefully a photomultiplier with a high quantum efficiency and with large gain. The electronic apparatus must be sensitive to pulses corresponding to one photoelectron from the photomultiplier cathode. The efficiency for different type FÉU-24 photomultipliers ranged from 40 to 96%.

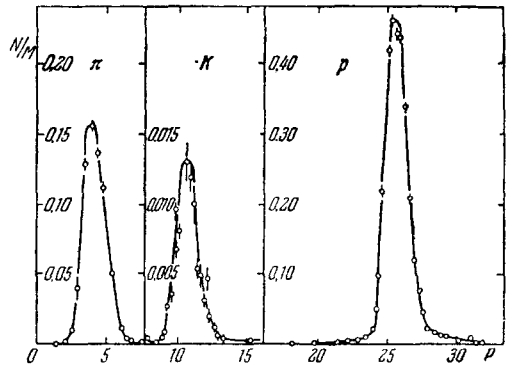

FIG. 26. Mass spectrum obtained with the aid of type D_4 counters in a beam of particles with momentum 4.75 BeV/c. Abscissa–ethylene pressure in atmospheres. Ordinates–ratio of the count of two D_4 to the scintillation monitor.

The background in the counters is approximately 2%. To separate K mesons ethylene was used instead of air to reduce the background. The resolution of the counter D_4 determined from curve Y_2 of Fig. 25b ($\Delta\beta/\beta \sim 10^{-3}$) is close to the theoretical value (7×10^{-4}).

Figure 26 shows an example of the mass spectrum of a beam of 4.75 BeV/c particles, obtained with the aid of two DGC connected for coincidence. The background in the K^- meson peak amounts to less than 1% of the count in the maximum. The diagram of the second differential counter D_5, obtained in the high-energy laboratory of the Joint Institute of Nuclear Research [64], is shown in Fig. 27. Its optical system consists of a spherical mirror with focal distance 110 cm and two parabolic mirrors, in the focus of which are located the cathodes of the photomultipliers. The reflecting surface of the parabolic mirrors serves simultaneously as a diaphragm. The internal surface of the counter is covered with black velvet. The working medium is ethylene. An experimental curve of the counter efficiency of the function of the glow angle of π^+ mesons with momentum 3.14 BeV/c is shown in Fig. 28. The counter velocity resolution calculated from this curve is $\Delta\beta/\beta = 5 \times 10^{-4}$.

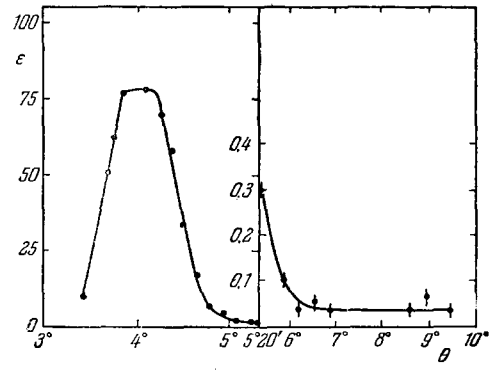

FIG. 28. Registration efficiency of D_5 counter to 3.14-BeV/c positive pions as a function of the glow angle.

FIG. 27. Diagram of the construction of the D_5 counter (dimensions in centimeters). 1–Duraluminum housing; 2–spherical aluminized mirror; 3–parabolic mirrors; 4–quartz windows (diameter 40 mm, thickness 20 mm); 5–FÉU-33 photomultipliers; 6–magnetic screen; 7, 8–duraluminum flanges 5 mm thick.

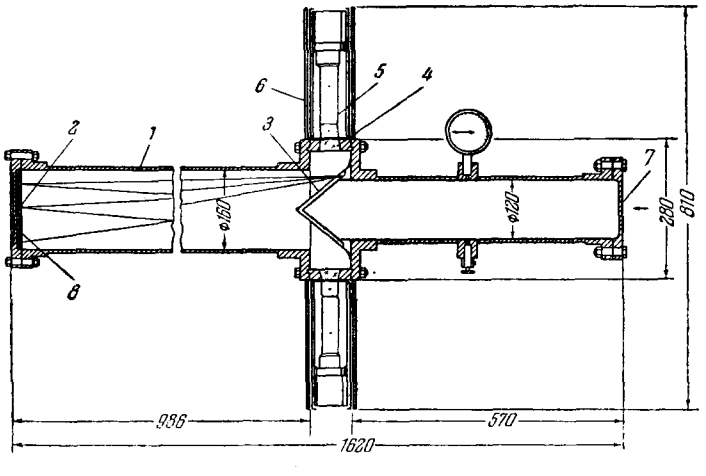

Thus, from among all the presently existing differential-counter constructions, the best velocity resolution $\Delta\beta/\beta = 3 \times 10^4$ is obtained in counter D_2, and this quantity agrees with the theoretical estimate determined essentially by the divergence of the beam.

The magnitude of the background in the DGC depends strongly on the sensitivity of the electronic apparatus. At high sensitivity $\varepsilon_b \sim 10^{-2}$. In order to obtain $\varepsilon_b \sim 10^{-3}$—$10^{-4}$, it is necessary to reduce the sensitivity of the apparatus, to a level corresponding to the production of dozens of photoelectrons on the photomultiplier cathode. Naturally, this decreases the efficiency of the counters at the maximum.

APPENDIX

Table I. Fraction of light (%) reflected at normal incidence from an opaque metallic film deposited on polished glass

Wavelength, Å	Chemically deposited silver	Sputtered aluminum	Wavelength, Å	Chemically deposited silver	Sputtered aluminum
1863	—	70	3160	4.2	—
1886	22	—	3261	14.6	91
1936	—	87	3380	55.5	—
1990	—	87	3404	—	83
2000	25	—	3570	74.5	—
2144	—	84	3610	—	84
2196	—	86	3850	81.4	90
2265	—	86	4200	86.6	—
2313	—	91	4500	90.5	91
2510	34.1	—	5000	92.0	92
2573	—	89	5400	93	—
2749	—	90	5500	92.7	—
2880	21.2	—	5800	94.8	—
2981	—	90	6000	92.6	92
3050	9.1	—			

Table II. Fraction of light P (%) reflected from a thin glass polished plate at different angles of incidence and for different refractive indices.

Angle of incidence θ, deg	P, %				
0	7.8	8.8	10.2	11.3	12.6
10	7.8	8.8	10.2	11.3	12.6
20	8.0	8.9	10.3	11.4	12.7
30	8.0	9.1	10.4	11.4	12.8
40	8.6	9.8	11.1	12.2	13.4
50	10.4	11.6	12.7	13.9	15.1
60	15.2	16.3	17.4	18.4	19.4
70	27.3	28.1	28.9	29.6	30.2
Refractive index	1.50	1.55	1.60	1.65	1.70

Table III. Transparency of fused quartz in the ultraviolet region of the spectrum [61] *

λ, mμ	Transparency, %	λ, mμ	Transparency, %
217	6.0	252	62.0
220	10.1	256	73.0
224	21.2	260	82.0
226	28.0	264	87.5
230	38.0	268	90.0
232	40.9	272	91.0
234	41.9	276	91.2
236	41.9	280	91.6
238	41.3	290	92.0
240	41.3	300	91.8
242	41.9	—	—
244	43.5	350	92.0
248	50.9	400	92.4

*The transparency of optical glasses in the ultraviolet region can be found in handbooks [62, 63].

Table V. Radiation length t_0 for different substances (see [67])

Element or substance	t_0, g/cm²	Element or substance	t_0, g/cm²	Remarks
Hydrogen	62.8	Silver . . .	9.0	
Helium	93.1	Iodine . . .	8.5	
Lithium	83.3	Xenon . . .	8.5	
Beryllium	66.0	Tungsten . . .	6.8	
Boron	53.6	Lead . . .	6.4	
Carbon	43.3	Air . . .	37.1	
Nitrogen	38.6	N—75.52% O—23.14% Ar—1.34%		
Oxygen	34.6			
Fluorine	33.4	Water	36.4	
Sodium	28.2	Clay (kaolin)	28.8	
Aluminum	24.3	Quartz, SiO_2	27.4	
Silicon	22.2	Limestone $CaCO_3$	24.2	
Chlorine	19.5			
Argon	19.7	Rock salt NaCl	22.2	
Potassium	17.4	Nuclear emulsion NIKFI-R	11.4	
Calcium	16.3			
Iron	13.9			
Copper	13.0	Plastic scintillator	44.4	
Bromine	11.5	LiH	80.0	
Ethane C_2H_6	46.1	Methyl fluoride CH_3F	38.05	$\frac{1}{t_0} = \sum_i \left(p_i / t_{0i} \right)$, where p_i—fraction by weight and t_{0i}—radiation length of the i-th component.
Methane CH_4	47.0	Nitrous oxide N_2O	37.05	
Propane C_3H_8	46.0	Nitric oxide NO	36.4	
Ethylene C_2H_4	45.3	Carbon monoxide CO	37.9	
Acetylene C_2H_2	44.4	Freon-13 $CClF_3$	27.5	
		Freon-12 CCl_2F_2	24.0	

Table IV. Refractive index of fused quartz as a function of the wavelength of the light (density of fused quartz $\rho = 2.21$ g/cm³)

n	1.4561	1.4564	1.4568	1.4585	1.4619	1.4632
λ, Å	6708	6563	5893	5461	5086	4861
n	1.4636	1.4697	1.4869	1.5339	1.5743	
λ, Å	4800	4047	3034	2144	1852	

Table VI. Explosive concentrations of gases mixed with air in local heating to ~500—600°C

Gas	Per cent in air
Hydrogen	4÷75
Ammonia	15.7÷27.4
Acetylene	2.3÷82
Ethylene	3÷33.5
Methane	5÷15
Ethane	3÷14
Propane	2.1÷95

[1] J. V. Jelley, Cerenkov Radiation and Its Applications, Pergamon, 1958.
[2] B. M. Bolotvskiĭ, UFN 62(3), 201 (1957). UFN 75, 295 (1961), Soviet Phys. Uspekhi 4, 781 (1962).
[3] Matulenko, Savin, and Stavinskiĭ, PTÉ no. 3, 44 (1956).
[4] Gilly, Leontic, Lundby, Meunier, Stroot, and Szeptycka, PICIP (Proc. of Int. Conf. on Instrum. for High-Energy Physics, Berkley, 1960.) p. 87.
[5] Ascoli, Balzanelly, and Ascoli, Nuovo cimento 10, 1345 (1953).
[6] Ascoli, Balzanelly, and Ascoli, Nuovo cimento 11, 562 (1954).
[7] Barclay and I. Jelley, Nuovo cimento 2, 27 (1955).
[8] K. G. Dedrik, Phys. Rev. 87, 891 (1952).
[9] B. B. Rossi and K. Greisen, Revs. Modern Phys. 13, 240 (1941).
[10] B. Rossi, High Energy Particles, Prentice Hall, 1952.
[11] M. V. Vol'kenshteĭn, Molekulyarnaya optika (Molecular Optics) Gostekhizdat, 1951.
[12] L. D. Landau, Phys. USSR 8, 201 (1944).
[13] Hill, Caldwell, Frisch, Osborn, Ritson, and Schluter, Rev. Sci. Instrum. 32, 11 (1961).
[14] Belyakov, Vovenko, Kirillov, Kulakov, Lyubimov, Matulenko, and Savin, PTÉ no. 1, 32 (1961).
[15] L. Koch, R. Lesueur, J. phys. radium 19, 103 (1958).
[16] W. Hartman and F. Berngard, Photomultipliers (Russ. Transl.) Gostekhizdat, 1961.
[17] R. Nobles, Rev. Sci. Instrum. 27, 280 (1956).
[18] I. Marshall, Phys. Rev. 86, 685 (1952).
[19] G. von Dardel, PICIP, p. 166.
[20] G. G. Slyusarev, Geometricheskaya optika (Geometrical Optics) AN SSSR, 1946.
[21] D. D. Maksutov, Astronomicheskaya optika (Astronomical Optics) Gostekhizdat, 1946.
[22] D. S. Volosov and M. V. Tsivkin, Teoriya i raschet svetoopticheskikh sistem (Theory and Design of Optical Systems), Iskusstvo, 1960.
[23] G. W. C. Kaye and T. H. Laby, Tables of Physical and Chemical Constants, Longmans, 1948.
[24] Intern. Critical Tables, vol. 7, McGraw-Hill, New York, 1950, p. 6—11.
[25] A. Tollestrup and W. Wentzel, Phys. Rev. 93, 950 (1954).
[26] B. Kinsey and W. Wentzel, CERN Symposium, Geneva, vol. 2, 1956, p. 68.
[27] S. Lindenbaum and L. C. L. Yuan, CERN Symposium, Geneva, vol. 2, 1956, p. 68.
[28] R. Hanson and D. Moor, Nuovo cimento 4, 1558 (1956).
[29] Beneventano, Agostino, Galtieri, Rispoli, Serra, Nuovo cimento 12, 156 (1959).
[30] J. Atkinson and V. Perez-Mendez, Rev. Sci. Instrum. 30, 864 (1959).
[31] R. Swanson and G. Masek, Rev. Sci. Instrum. 32, 212 (1961).
[32] A. Babev and L. Landsberg, PTÉ no 6, 40 (1960).
[33] G. Hutchinson, Prog. Nucl. Phys. 8, 195 (1960).
[34] Baldwin, Burrowes, Caldwell, Hamilton, Hill, Osborn and Ritson, IRE Trans. Nucl. Sci., No. 3—5, 117,(1958).
[35] Deutsch, Intern. Conf. on High-Energy Acceler. and Instr., CERN, Geneva, 1959, p. 593.
[36] Burrowes, Caldwell, Frisch, Hill, Ritson, Schluter, and Wahling, Phys. Rev. Letts. 2, 119 (1959).
[37] Burrowes, Caldwell, Frisch, Hill, Ritson, and Schulter, Phys. Rev. Letts. 2, 117 (1959).
[38] Mermod, Winter, Weber, and von Dardel, PICIP, p. 172.
[39] Cork, Keefe, and Wentzel, PICIP, p. 84.
[40] Armenteros, Coombs, Cork, Lambertson, and Wentzel, Phys. Rev. 119, 2068 (1960).
[41] Cook, Cork, Hoang, Keefe, Kerth, Wentzel, and Zipf, Phys. Rev. 123, 320 (1961).
[42] Likhachev, Lyubimov, Stavinsky, and Chzan, PICIP, p. 89.
[43] Vovenko, Kulakov, Likhachev, Lyubimov, Matulenko, Savin, and Stavinskiĭ, PTÉ, no 2, 50 (1962).
[44] Spravochnik po razdeleniyu gazovkykh smeseĭ (Gas Mixture Separation Handbook), Goskhimizdat, 1953.
[45] Spravochnik po glubokomu okhlazhdeniyu (Deep Cooling Handbook), Gostekhizdat, 1947.
[46] M. Vukalovich and I. Novikov, Uravneniya sostoyaniya real'nykh gazov (Equations of State of Real Gases), GEI, 1948.
[47] E. Gauss, Rev. Sci. Instrum. 32, 164 (1960).
[48] B. F. Dodge, Chemical Engineering Thermodynamics, McGraw Hill, 1944.
[49] Teplofizicheskie svoĭstva veshchestva (Thermophysical Properties of Matter), (Handbook), Gosenergoizdat, 1956.
[50] Thermodinamic Function of Gases, Ed. by F. Din, London, 1961.
[51] I. Baldykes, Rabochie veshchestva kholodil'nykh mashin (Working Media for Refrigerators), Pishchepromizdat, 1952.
[52] Bhiday, Jenninga, and Kalmus, Roc. Phys. Soc. 72, 973 (1958).
[53] Vovenko, Golovanov, Kulakov, Matulenko, Lyubimov, Savin, and Smirnov, JETP 42, 715 (1962), Soviet Phys. JETP 15, 498 (1962).
[54] Vovenko, Kulakov, Matulenko, Likhachev, Lyubimov, Savin, Smirnov, Stadinskiĭ, Chang, and Hsu, Preprint, Joint Inst. Nuc. Res. D-721, 1961.
[55] S. Friberg, J. Phys. Chem. 1326, 195 (1934).
[56] S. Friberg, J. Phys. Chem. 41, 378 (1927).
[57] J. Koch, Matem. Astr. och. Fys. 8, No. 20 (1912).
[58] J. Koch, Matem. Astr. och. Fys. 10, No. 1 (1914).
[59] J. Koch, Matem. Astr. och. Fys. 18, No. 3 (1924).
[60] J. Koch, Matem. Astr. och. Fys. 9, No. 6 (1913).

[61] V. P. Pryanishnikov, Kvartsevoe steklo (Quartz Glass) Promstroĭzdat, 1956.
[62] Katalog tsvetnogo stekla (Colored Glass Catalog), No. 106, Oborongiz, 1959.
[63] Supplement to Colored Glass Catalog No 106, Oborongiz, 1959.
[64] M. Likhachev and V. Stavinsky, Nucl. Instr. 20, 261 (1963).
[65] Lindenbaum, Love, Niederer, Ozaki, Russell, and Yuan, Phys. Rev. Letts 7(5), 185 (1961).
[66] Vivargent, von Dardel, Mermod, Weber, and Winter, Preprint, CERN.
[67] O. I. Dovzhenko and A. A. Pomanskiĭ, JETP **45**, 268 (1963), Soviet Phys. JETP **18**, 187 (1964).

Translated by J. G. Adashko